Surface Plasmon Resonance Biosensor Based on Graphene Wrapped Cysteine Self-assembly for Cardiac Troponin I Detection

The project report in partial fulfilment of the requirement for the degree of

Master in Technology

In

Industrial Biotechnology

Submitted by

Divya Rani Dubey
Roll Number: 2k14/IBT/04
Under the supervision of
Prof. B. D. Malhotra

Department of Biotechnology

Delhi Technological University,

Delhi-110042 (India)

DECLARATION

Certified that the project report entitled ”Surface plasmon resonance biosensor based on graphene wrapped cysteine self-assembly for cardiac troponin I detection,” submitted by me is in partial fulfilment of the requirement for the award of the degree of Master of Technology in Industrial Biotechnology (IBT), Delhi Technological University (DTU). It is a record of original research work carried out by me under the supervision of Prof. B.D. Malhotra, Department of Biotechnology, Delhi Technological University (DTU), Delhi-110042. The matter embodied in this project report is original and has not been submitted for the award of any other degree/ Diploma.

Date:

Divya Rani Dubey
Roll No. 2k14/IBT/04
Department of Biotechnology
Delhi Technological University
Delhi-110042

CERTIFICATE

This is to certify that the project entitled "Surface Plasmon Resonance Biosensor Based on Graphene Wrapped Cysteine Self-assembly for Cardiac Troponin I Detection**"** submitted by Ms. Divya Rani Dubey (Roll No. 2k14/IBT/04) in the fulfilment of the requirements for the reward of the degree of Master of Technology, Delhi Technological University, Delhi-110042 is an authentic record of the candidate's own work carried out by her under my guidance. The information and data enclosed in this synopsis is original and has not been submitted elsewhere for honouring of any other degree.

Prof. B. D. Malhotra
(Project Mentor)
Department of Bio-Technology
Delhi Technological University
Delhi-110 042

Prof. D. Kumar
Professor, Head of Department
Department of Bio-Technology
Delhi Technological University

ACKNOWLEDGEMENT

I hereby express my profound sense of reverence of gratitude to my mentor Prof. B. D. Malhotra, Department of Biotechnology, Delhi Technological University, Delhi-110042 for his valuable guidance, congenial discussion, incessant help, calm, endurance, constructive criticism and constant encouragement throughout these investigations right from the imitation of work to the ship shaping of the project report.

I express my kind regards and gratitude to Prof. D. Kumar, Head of Department (HOD), Department of Biotechnology, Delhi Technological University, Delhi for his interest and encouragement at various stages.

I am highly indebted to Dr. Chandra Mouli Pandey, Mr. Saurabh Kumar, Mr. Suveen Kumar and Ms. Shine Augustine for their guidance and constant supervision as well as for providing necessary information regarding the instruments and experiments and also for their support in completing the report.

I would also like to express my sincere thanks to the members of National Physical Laboratory (NPL), Delhi; especially Shipra Solanki and M.K.Pandey for helping in lab work and their much needed cooperation.

I am also thankful to all the staff members of the department of Biotechnology, DTU; especially Mr. Chail Bihari, Mr. Jitendra Singh and Mr. Mukesh Kumar for providing necessary chemicals and maintaining laboratory in good working conditions.

I have no word to express my deep sense of gratefulness and affection to all my family members and friends for their continuous love, support, encouragement, and of course persuasion to continue to study and understand the true value of education and the rewards of perseverance.

Last but not the least, thanks to all other who have not been mentioned by name but they have given invaluable helps and encouragement.

Divya Rani Dubey
2K14/IBT/04
M.Tech. (IBT)

CONTENTS

Topics **Page No.**

List of Abbreviations

A Ampere

Ab Antibody

Ag Antigen

AMI Acute myocardial infarction

Au Gold

BSA Bovine serum albumin

CE Counter electrode

Cys Cysteine

cTnI Cardiac troponin I

CV Cyclic voltammetry

CVD Cardiovascular disease

Da Dalton

DI Deionized

DNA Deoxyribonucleic acid

Epa Anodic peak potential

Epc Cathodic peak potential

EDC N'- ethyl -N- (3-dimethylaminopropyl) carbodimide

EIS Electrochemical impedance spectroscopy

$[Fe(CN)_6]^{4-}$ Ferrocyanide

$[Fe(CN)_6]^{3-}$ Ferricyanide

FTIR Fourier transform infrared spectroscopy

GO	Graphene oxide
GOx	Glucose oxidase
Ipa	Anodic peak current
Ipc	Cathodic peak potential
NHS	N-hydroxysuccinamide
PBS	Phosphate buffer saline
R_{CT}	Charge transfer resistance (Nyquist diameter)
rGO	Reduced graphene oxide
SAM	Self assembled monolayer
SEM	Scanning electron microscopy
SPR	Surface plasmon resonance
TEM	Transmission electron microscopy
V	Volt

List of Tables

List of Schemes/Figures

Figure 5.9	Cyclic voltammogram (CV) studies of rGO-Cys/Au electrode as a function of scan rate (10-250 mV/s), Inset (a) shows the magnitude of oxidation and reduction current generated as response of scan rate (mV/sec), Inset (b) shows the potential as a function of scan rate.
Figure 5.10	CV studies of BSA/anti-cTnI/rGO-Cys/Au bio-electrode as a function of scan rate (10-300 mV/s), Inset (a) magnitude of oxidation and reduction current generated as response as a function of scan rate (mV/sec), Inset (b) potential as a function of scan rate.
Figure 5.11	EIS response plot of BSA/anti-cTnI/rGO-Cys/Au electrode as a function of cTnI concentration (1-80ngmL^{-1}) in 5 mM [Fe $(CN)_6]^{3-/4-}$ PBS solution at pH 7.4.
Figure 5.12	EIS linearity plot showing the response of BSA/anti-cTnI/rGO-Cys/Au electrode with increasing concentration of cTnI ranging from 1-80 ngmL^{-1} in PBS solution (pH 7.4) containing 5mM [Fe $(CN)_6$]$^{3-/4-}$.
Figure 5.13	Graph between ΔRct/Rct(co) and the concentration of cTnI for calculating association constant (Ka) of anti-cTnI/rGO-Cys/Au electrode.

CHAPTER-1

Abstract

Surface plasmon resonance biosensor based on graphene wrapped cysteine self-assembly for cardiac troponin I detection

Divya Rani Dubey

Delhi Technological University, Delhi, India

Email Id: divyadubey09@gmail.com

1. Abstract

This dissertation contains results of the studies related to the fabrication of a label free biosensor based on reduced graphene wrapped cysteine (rGO-Cys) self assembled on gold (Au) electrode for the detection of cardiac troponin I (cTnI) using electrochemical and surface plasmon resonance (SPR) techniques. The rGO-Cys were characterized using transmission electron microscopy, scanning electron microscopy, Fourier transform infrared spectroscopy (FT-IR) and contact angle (CA) measurements. Further, SPR studies were used to investigate the immobilization process and the binding kinetics of antigen-antibody interactions and it was observed that 11.7ng of anti-cTnI has been immobilized on the surface of Au electrode under optimized conditions. The response studies carried out using electrochemical impedance spectroscopy shows that the fabricated bio-electrode has sensitivity of 0.0642Ω $mLng^{-1}cm^{-2}$, linear detection range of 1-80 $ngmL^{-1}$, linear regression coefficient of 0.9956 and lower detection limit of 0.0697 $ngmL^{-1}$.

Keywords: reduced graphene oxide (rGO), cysteine (Cys), cardiac troponin-I (cTnI), self assembled monolayers (SAMs), surface plasmon resonance (SPR), electrochemical impedance spectroscopy (EIS).

CHAPTER-2

Introduction

2. Introduction

Cardiovascular diseases (CVDs) occur under chronic medical conditions and necessitate its early diagnosis. It has been estimated that the number of deaths are likely to increase to 23 millions per year due to CVDs (Fathil et al. 2015). Acute myocardial infarction (AMI) is one of the cardiovascular diseases in which the heart muscles get damaged due to the reduced supply of oxygen or glucose from the coronary artery. It happens due to the narrowing of arteries that leads to blood flow restriction (Pawula et al. 2016). Several cardiac biomarkers have been investigated for the detection of AMI such as creatine kinase, myoglobin, cardiac troponin I (cTnI) and cardiac troponin T (Fathil et al. 2015). The cTnI is considered to be as one of the most reliable biomarkers for the detection of AMI because of its specificity towards cardiac tissue injury (Lum et al. 2006). When the cardiac tissue injury occurs, cTnI is released into the blood serum within 3-4h and its concentration increases from ~0.001µg L^{-1} (healthy person) to a value as high as ~100 µg L^{-1} (Fathil et al. 2015). The cTnI biomarker provides a long window for detection as its level return to normal range only after 4-10 days (Ahammad et al. 2011).

The traditional diagnostic clinical methods for AMI detection include immunoassays (ELISA or RIA), equilibrium dialysis, affinity chromatography and spectroscopic techniques (Zapp et al. 2014). These conventional techniques can be used to detect different biomarkers specific for cardiac injury via labeling technology. The drawbacks of these conventional techniques are labor-intensive, time consuming and expensive. In this context, biosensors provide advantages over these traditional techniques such as rapid detection, inexpensive diagnostics, label free detection, rapidity and low reagent consumption (Kumar et al. 2015). Bio-sensing platform holds path breaking potential to emerge as a global key player in the field of healthcare and diagnostics.

In recent years, surface plasmon resonance (SPR) based biosensors have been widely explored in the field of biosensors. SPR based biosensor measures the changes in refractive index that takes place upon hybridization and it provides a signal that can be directly correlated with the mass density changes on a metal surface. SPR holds several advantages over other conventional techniques such as monitoring of binding events in real time, label-free detection of biochemical interactions, resolving kinetics and mechanism of bio-molecular interactions etc (Matharu et al. 2009). The information obtained from the binding curves are known to provide rich information on specificity, affinity, kinetics of biomolecular interactions and the concentration of analyte of interest in a complex sample. The immobilization of given proteins on various matrices such as membrane entrapment, conducting polymers, self assembled monolayer (SAM) etc are possible for the fabrication of SPR based biosensors.

Among the various matrices, the use of SAMs are widely explored due to its unique properties which include easy manipulation of functional groups through various chemistries, biocompatibility with bio-molecules, help in controlling over the biomolecular orientation on the surface, facilitating electron transfer at the interface of bio-molecules and surface of electrode (Campuzano et al. 2002; Nakaminami et al. 1999).

Application of nano-composites with multi-functional properties has tremendous potential for biosensor designing and these nano-composites have interesting properties such as good conductivity, large surface area and permeability due to their spatial arrangement and size dependent properties. In this regard, the fabrication of micro structures by combining two-dimensional graphene with nanoparticles has gained much interest of researchers due to the properties it holds such as high electrical/thermal conductivity, chemical stability, large surface area and brilliant mechanical properties. Although GO structures have extended the range of its applications but the major drawback is the use of chemical reducing agents

required for the chemical reduction process from GO to rGO usually leads to environmental health risks. There is thus considerable need for developing an eco-friendly biomaterial that is biocompatible and have high electron transfer efficiency.

Recently developed green synthesis method has been used for the development of new generation of nanomaterials by utilizing the template of cysteine (Cys). In this present work, GO is added into the cysteine solution (pH 8) and is kept for sonication at 25°C overnight. Self assembly of this synthesized nanocomposite showed excellent electrochemical properties onto Au substrate.

We have fabricated an SPR based assay for the detection of cTnI marker by immobilizing anti-cTnI on the self assembly of rGO-Cys at Au surface. The modified rGO-Cys/Au sensor disk is employed as the sensor platform for the cTnI detection.

CHAPTER-3

Literature Review

3. Literature Review

3.1 Cardiovascular Diseases

The Cardiovascular diseases (CVDs) belong to a class of diseases that can cause adverse affect on the heart or blood vessels and globally these diseases are the leading cause of death. It has been estimated that in 2008, 30% of all global deaths were due to cardiovascular diseases and by 2030 it is estimated that 23 million deaths each year are likely to be due to CVDs (Fathil et al. 2015). Acute myocardial infarction (commonly known as a heart attack) is one of cardiovascular diseases (Pawula et al. 2016). Injury to a part of heart muscle results into AMI and this leads to the reduction in blood supply due to the blockage in coronary artery (Fathil et al. 2015). The early diagnosis and immediate treatment to AMI have become necessary to increase the survival rate. Treatment to the disease at early stage is vey essential as delayed treatment increases the probability of mortality.

3.2 Conventional diagnostic techniques

The traditional methods to diagnose the disease are pursued by monitoring the increased level of AMI specific biomarkers in blood serum. Conventional clinical diagnostic techniques for cardiac troponin I detection include immunoassays of specific biomarkers with labelling technology such as enzyme-linked immunosorbent assay (ELISA) and radioimmunoassay (RIA). Several cardiac biomarkers such as myoglobin, creatine kinase MB (CK-MB), cardiac troponin I (cTnI) and myeloperoxidase (MPO) (Fathil et al. 2015) have been reported. Among all these biomarkers, cardiac troponin I has been recognized as a gold standard because it is highly specific and sensitive to acute myocardial cell injury (Lum et al. 2006). Troponin is a complex of three regulatory proteins troponin C, troponin T and troponin I that are present in each myofibril of muscle fibers of cardiac muscles. However cardiac troponin I is an integral protein of molecular weight 24kDa (isoelectric point ~9.9) controls the calcium mediated interaction between calcium and myosin (Jagadeesan et al.

2012). The drawbacks of adopting these conventional approaches include multistep processing of samples, require long time and are expensive (Kong et al. 2012). To overcome these drawbacks, biosensors offer several advantages such as label free detection, less diagnostic time, flexibility and reliability.

3.3 Biosensor

According to the International Union of Pure and Applied Chemistry (IUPAC), biosensor is a self contained integral device that is capable enough to provide quantitative analytical information using a biological element. Biosensor incorporates biological recognition element which allows specific interaction with the target analyte, and the obtained signal is measured by transducer present in the close vicinity of biological recognition element. Several biomolecules like antibodies, enzymes, nucleic acids, receptors proteins, cells or tissues can be used as biological elements for biosensing processes. The biosensing devices possess several properties such as high specificity, rapid detection, flexibility, reliability and low cost that can bring development in healthcare and environmental monitoring sector. Enzyme based biosensor was the first biosensing platform developed by Clark and Lyons to detect the concentration of glucose in blood serum in the year 1962. This fabricated biosensor detects the amount of oxygen consumed during the reaction between the thin layered glucose oxidase (GOx) entrapped over oxygen electrode through semi permeable membrane. The chemical equation given below shows the working of fabricated enzyme based biosensor.

$$\text{Glucose} + O_2 \longrightarrow \text{gluconic acid} + H2O2 \qquad \text{.....Eq. 3.1}$$

After the discovery of this biosensor, a lot of work has been done towards the development of the biosensors for healthcare and environmental applications. Modifications have been made in the components of the biosensor which include biological recognition element, immobilization matrix, transducer (Figure 3.1).

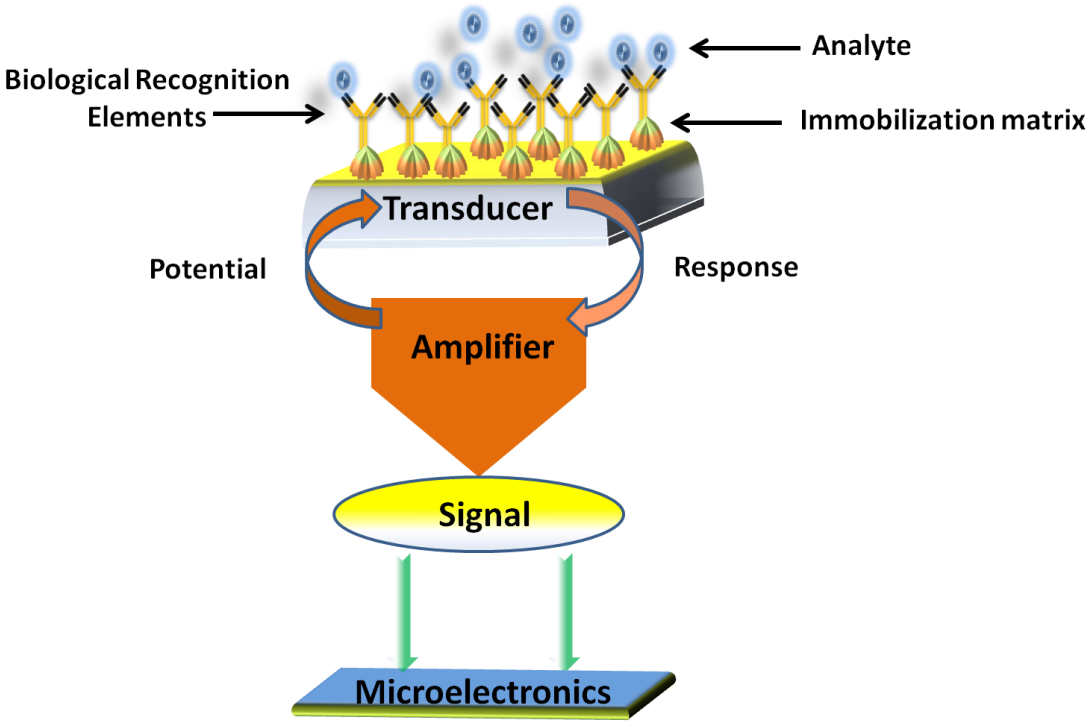

Figure 3.1 shows various components of a biosensor.

3.3.1 Biological recognition elements

The biological recognition elements or bioreceptors can be categorized into two different groups i.e. catalytic and non-catalytic. The catalytic group includes enzymes, plant or mammalian tissue and micro-organisms while the non-catalytic class includes antibodies, nucleic acids and receptors. The output generated through the interaction is detected by transducer.

3.3.2 Immobilization matrix

An Immobilization matrix provide support to desired biomolecules for the immobilization process to occur at the surface of transducer and at the same time can be utilized for maintaining stabilized environment for biomolecules in order to retain their

biological functions for a longer period of time. The selection of immobilization method depends on the chemical properties of desired solid support which may includes ionic strength, chemical composition, physiological pH etc. Several techniques such as physical adsorption, chemisorptions, membrane entrapment, etc, have been used to immobilize the biomolecules on the matrices. The physical methods of immobilization suffer several shortcomings such as long incubation time, non- reproducible results due to leaching of bio-molecules at the time of washing. Compared to physical adsorption technique, the covalent method is more reliable covalently bound biomolecules on the solid surface are highly stable and also lead to reduction in non-specific binding. For the immobilization process various kinds of matrices such as self assembled monolayers (SAM), nanomaterials, sol gels, and conducting polymers can be utilized. Among these matrices, SAMs have recently gained much interest in biosensors application. This is due to their unique properties which include biocompatibility with the biomolecules, easy manipulation of biological and organic properties by changing functional groups on SAM, highly stable, simple and provides orientation to the biomolecules.

3.3.3 Transducers

Transducers are the physical components of the sensor that generates signal due to the interaction taking place between the biological sensing element and the target analyte. When analyte are specifically recognized by the biological element then signal generated which is converted into measurable signal by the transducers. The biosensors on the basis of transducers are categorised into three broad categories such as electrochemical biosensor (Ghindilis et al. 1998), piezoelectric biosensor (Chu et al. 1995) and optical biosensor (Gauglitz 1996).

3.3.3.1 Electrochemical biosensor:

The electrochemical biosensors have been developed for detection of several biomarkers present in blood serum, saliva, sweat and urine etc. They basically involved the use of electrochemical species which undergoes consumption or generation during a biological and chemical process of an analyte and substrate. The interaction results into an electrochemical signal which is simultaneously monitored by an electrochemical analyser. On the basis of electrochemical property, biosensors are categorised into three subheads:

3.3.3.1.1 Potentiometric biosensor:

This biosensor measures the potential at the working electrode with respect to reference electrode and then measures the charge generated through selective biomolecular binding at the electrode surface.

3.3.3.1.2 Amperometric biosensor:

This biosensor measures signal based on the linear relationship exists between analyte concentration and current. Change in current occurring due to the direct oxidation of the biomolecular species present on the working electrode is measured. The sensor potential is fixed at particular value and the current is produced through analyte directly or indirectly at the electrode. These biosensors show cost effectiveness, high sensitive and rapidity.

3.3.3.1.3 Conductometric biosensor:

This device consists of two noble metal electrodes, which are immersed in the solution and the conductance is measured. Some enzymatic reactions convert neutral substrates into charged products, causing a change in the conductance of the medium. Although this transducer is not in widespread use, the technique is routinely used to measure salinity of marine environments. The main advantages of electrochemical biosensors are simplicity, fast response time and low cost.

3.3.3.2 Piezoelectric biosensors:

In this biosensor, the resonance frequency changes during biomolecular interaction which can be converted into an electrical signal proportional to the amount of analyte present. The piezoelectric biosensor not only offers ease of use, real-time output but also provide a wide pH range for working (Chu et al. 1995).

3.3.3.3 Calorimetric biosensors:

The calorimetric biosensors are based on the heat generated during biochemical reaction between analyte and sensing biomolecule. Most of heat evolved during a chemical reaction is lost into the surrounding medium without being detected; this biosensor is not sensitive enough to produce accurate results.

3.3.3.4 Optical biosensor:

Optical biosensors are based on optical principles for the transduction of a biochemical interaction into a readable output signal. The biomolecular interaction on the sensor surface modulates the light characteristics of transducer (i.e intensity, phase, polarisation, etc.) and the biosensing event can measured by the change in diverse optical properties such as absorption, fluorescence, luminescence or refractive index. Optical biosensors have several advantages such as multiple analyte detection at a time with different wavelength, in vivo application.

3.4 Surface Plasmon Resonance biosensor

The surface plasmon resonance (SPR) biosensor are optical sensors involving electromagnetic waves (surface plasmon) to detect biomolecular interactions between an immobilized biomolecular recognition element on the SPR sensor surface and an analyte in solution (Homola 2003). SPR based biosensors are gaining much interest due to its label-free optical biosensing technologies and can be used in important areas including medical diagnostics, environmental monitoring, food safety, and security. The important feature of

SPR based biosensor is to study macromolecular interactions with high stability, reduced number of non-specific interactions, flexibility and use of reproducible immobilization technique. SPR based biosensor contains either a bare gold disk or modified gold layers of thickness 40-50nm to perform kinetic measurements and to study interactions such as protein-protein (Karlsson and Fält 1997), protein-ligand (Jung et al. 2000), enzyme-substrate, DNA-DNA interaction (Moon et al. 2010; Sigal et al. 1996). The main drawback of this technique is complexity, high cost and large size (Matharu et al. 2009).

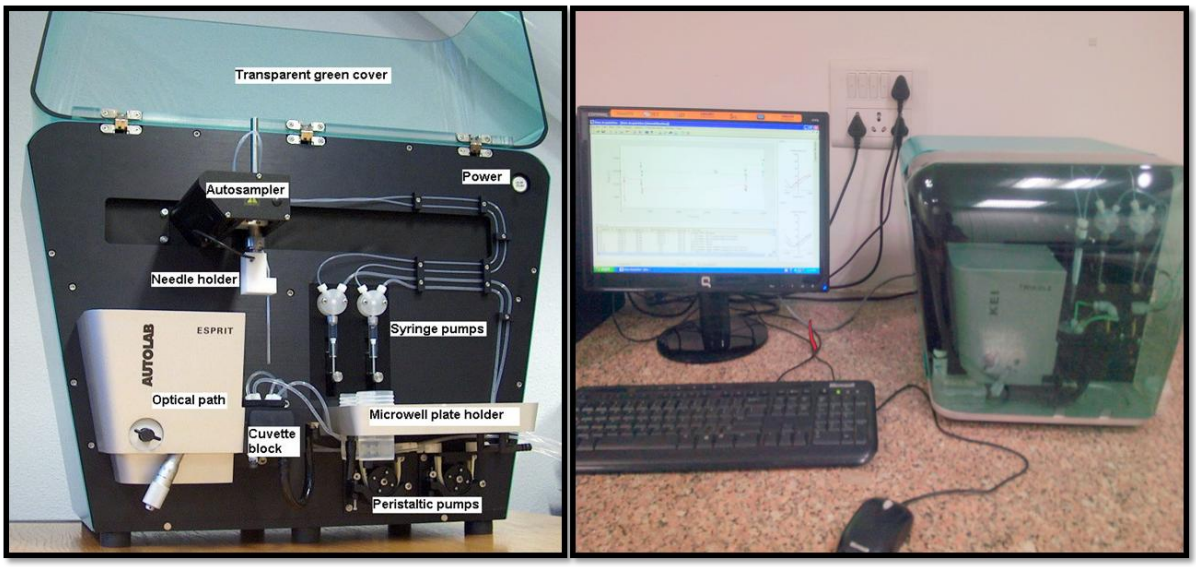

Figure 3.2 SPR instrument: The KEI Twingle.

3.4.1 Definition of surface plasmon resonance (SPR)

In 1968, SPR was first demonstrated by Otto but failed to make it commercially available. Later, Biacore® (GE Healthcare) have made efforts to bring the technique for its biomolecular interaction application in the real world (Daghestani and Day 2010; Otto 1968). SPR is defined by consistent fluctuation of longitudinal charges at the surface of a metal result in surface plasmon generation that have their intensity maximum at the surface and exponentially decaying field perpendicular to it. The surface plasmon is a p (plane)-polarized

surface bound electromagnetic wave propagating at the interface between a metal and a dielectric.

3.4.2 Working principle of SPR

Under certain conditions, SPR occurs when a thin film of metal (gold or silver) is placed inside the laser beam. When the incoming light is monochromatic and p-polarized (i.e. the electric vector component is parallel to the plane of incidence), the free electrons of the metal will oscillate and absorb energy at a certain angle of incident light. The angle of incidence at which SPR occurs is called the SPR angle. SPR can be detected by measuring the intensity of the reflected light. It can be observed that a sharp decrease or 'dip' in intensity is measured at the SPR angle. The position of the SPR angle depends on the refractive index in the substance with a low refractive index, i.e. the sensing surface (Daghestani and Day 2010). The refractive index of the sensor surface changes upon binding of macromolecules to the surface (Arya et al. 2006). As a result, the SPR wave will change and therefore the angle will change accordingly. Linear relationship between the amount of bound material and shift in SPR angle can be observed during the experimental analysis. The macromolecular binding to the surface can be quantified by measuring the SPR angle shift in millidegrees. A change of 122 millidegrees represents a change in surface protein of approximately 1 ng/mm^2, or in bulk refractive index of approximately 10^{-3}(Dian-Ping Tang et al 2006). The detection principle has one limitation which defines that the molecular weight of the analyte below 1000Da upon binding to the surface will show response that is too low to be detected directly. The size of particles or biomolecules can also be studied through the penetration depth of the evanescent wave (300-400 nm) (Daghestani and Day 2010; E 1971). When the size of particles is around 400Da then the linear relation between the response signals to the amount of bound particles is not generated. In this case, it becomes impossible to perform quantitative or kinetic analysis but the study of molecular binding can be done qualitatively.

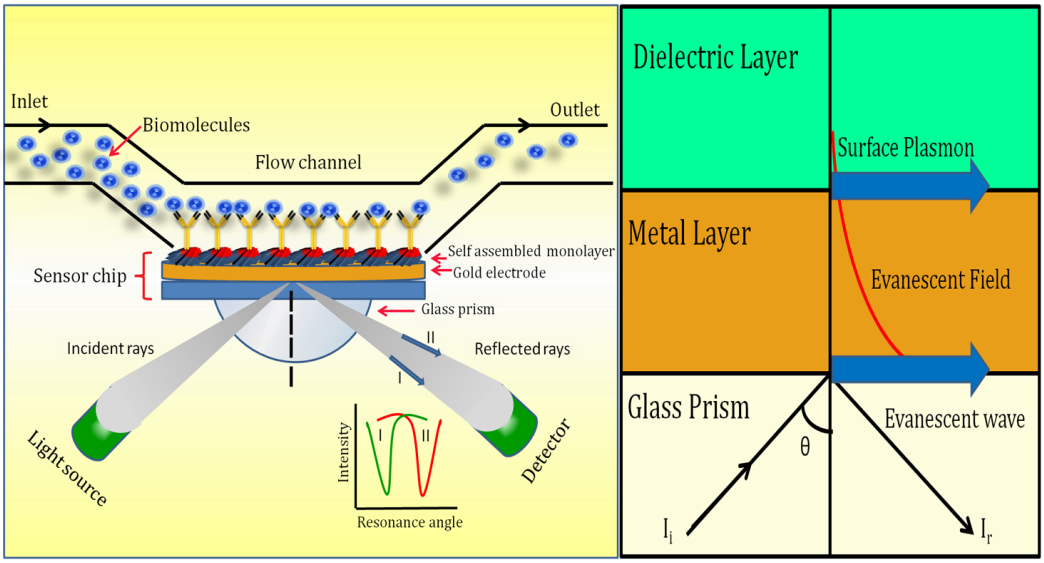

Figure 3.3 shows working principle of surface plasmon resonance (SPR)

In the SPR, a replaceable glass disk is used and coated with a thin gold layer on the hemi-cylinder. A thin layer of oil is applied between the disk and the hemi cylinder having same refractive index. This allows the light to reach the Au layer while passing through the hemi-cylinder, the oil and the glass. This results into the total internal reflection as the photons hit the gold instead of air. There is a special situation for the photons when a dielectric medium is placed on top of the gold. If the dielectric medium has an opposite (or higher) dielectric constant than gold, then the free electrons present on the gold will fluctuate and leads to charge fluctuations in the metal. Due to the thin metal layer, fluctuation of charges are taking place at the surface only and leads to an electromagnetic surface wave called as surface plasma oscillations. When light is incident at the gold surface under a certain angle of incidence, the energy of the photon interact with the free fluctuating electron and get excited which leads to surface plasmon resonance. Therefore, in total internal reflection situation the energy of the light is ideal (SPR situation) and the photons are converted to (resonating) plasmon so there will be very low light to be detected by the

detector. By plotting the light intensity versus angle of incidence will give a dip at the specific SPR angle. An incoming light beam is being reflected and detected by the detector and at a certain angle the reflected light intensity is decreased, at this point the surface plasmon resonance effect occurs.

The advantage of the SPR based biosensor lies in the label-free detection of the interactions which is mostly achieved by immobilization of the biomolecules onto the gold (Au) substrate. Several bio-functionalization techniques have been adopted for the immobilization of bio-recognition element onto the bio-electrode surfaces including covalent binding through self-assembled monolayers (SAMs), non-covalent membranes, and electro-deposition with conductive polymers. These methods lead to overcome the drawback of biomolecules when bound directly on bare electrode which results into the loss of their activity due to strong adsorption. Self assembled monolayer (SAM) can be utilized as immobilization matrices, as they allow control over dimensions and their end group biological and organic properties by easy manipulation of the functional groups by using different chemistries and thus it can become compatible for bio-molecules (Pandey et al. 2014b).

3.5 Self assembled monolayers

Self-assembled monolayers (SAMs) are organized, chemically and thermally stable two dimensional (2D) aggregates that are formed spontaneously through the process of adsorption of surface active molecules onto a solid substrate. The surface active molecules consist of a head group and it should be suitable for strong interactions or even chemical bonding with the surface. It also consist of a molecular backbone moiety which is responsible for 2D packing and provide favourable lateral interactions with the next neighbours and a tail or end group determining the properties of the newly formed solid surface.

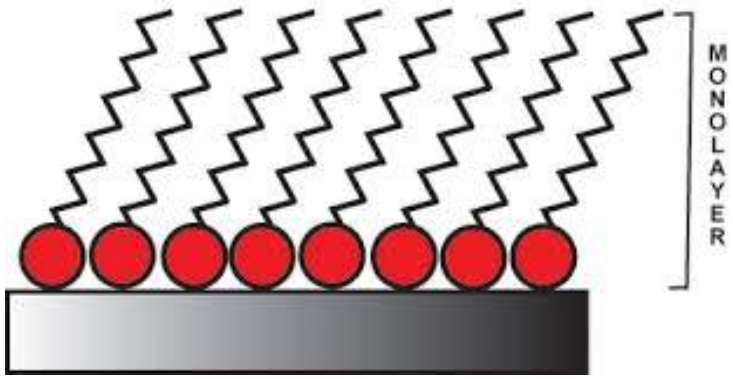

Figure 3.4 Scheme showing the formation of self assembled monolayer (SAM).

SAMs are particularly suitable towards developing applications in the area of biosensors because of their several unique properties which include stability, uniform surface structure and relative ease of manipulating functional groups (Nakaminami et al. 1999) (Campuzano et al. 2002). In addition to this, SAMs also provide stable biocompatible platform for biomolecular interactions and prevent non specific adsorption of biomolecules during immobilization at the electrode surface (Gu et al. 2002) (Frederix et al. 2003).

3.5.1 Formation of SAMs

The bare surfaces of metals and metal oxides tend to adsorb organic materials to form SAMs as these adsorbates lower the free energy of an interface between metal/metal oxide and the ambient environment. These two types of monolayers are highly robust as they provide strong bonding between the head groups and substrates. Ordered monolayers can be formed by using a very dilute solution whereas a high concentration with increased time favours multilayer formation. Dense coverage of adsorbates are obtained quickly from millimolar solutions (milliseconds to minutes), but a slow reorganization process requires controlled time interval to maximize the density of molecules and to reduce the defects.

3.5.2 Factors affecting SAM Formation and Stability

There are a number of factors that are known to affect the formation of a SAM and these parameters include temperature, adsorbate concentration, time of solvent immersion, adsorbate purity, concentration of oxygen in solution, substrate roughness, packing density and the rate of formation of a SAM. Defects formed in a monolayer can be controlled during the SAM formation at the surface of clean and smooth substrate like Au.

3.5.3 Surface modification for biosensor application

For applications in biosensor assembly, functionalized SAMs containing the bonds of thiol or silane can be synthesized. Modified SAMs can result in the development of surfaces with large/complex ligands and molecules needed for biochemical applications. Also the modification of the exposed surface on the SAM after formation offers many advantages which include simplicity to functionalized surfaces, stability, efficiency, manipulation of multifunctional groups at the SAMs via different chemistries etc. Modification of SAMs for designing biosensor can be done by adopting various methods as follows:

3.5.3.1 Physical Adsorption:

Physical adsorption is the easiest method for modifying the SAM. It is based on the interaction of charges present on the surface and molecules under desired conditions. It provides a method to study direct electron transfer between a bio-molecule's reaction site and the electrode surface. It also provides the opportunity to fabricate a multilayer electrode using ionic electrolytes with precise control over layer thickness.

3.5.3.2 Chemical Modification Using Activators:

Binding of bio-molecules using chemical activators has shown great potential for the development of commercial biosensors due to stability of the resultant bond. Chemical modification of SAM can be done by using various activators such as and N-hydroxysuccinimide (NHS) and N-ethyl-N'-(3-dimethylaminopropyl) carbodimide (EDC).

The use of EDC/NHS chemistry is widely employed for chemical modification in the fabrication of biosensor.

3.5.3.3 Chemical Modification Using Cross Linkers:

Binding of bio-molecules using cross linkers is another approach of chemical modification and can be achieved using compounds like 4-fluoro-3-nitroazidobenzene (FNAB), glutaraldehyde, biotin-avidin coupling etc. Immobilization of biomolecules such as antibodies, receptors, enzymes or DNA onto solid supports is a key step in assembly of biosensors or bioelectronic systems. Pandey et al. have fabricated an electrochemical genosensor based on the self assembly of 1-fluoro-2-nitro-4-azidobenzene (FNAB) decorated with octadecanethiol (ODT) for the detection of pathogenic bacterium *Escherichia coli.* They reveal that the sensitivity of their fabricated biosensors is 0.5 X 10^{-18} M with stability of four months (Pandey et al. 2011).

Self assembled monolayer (SAM) of thiols, silanes and disulfides at the surface of Au has emerged as a potential candidate to fabricate electrochemical biosensors via biomolecular immobilization (Frederix et al. 2003) (Fan et al. 2003). They provide homogeneous and well defined substrates properties that can control desired solid surface.

Self assembly of cysteine microstructures has recently attracted much interest for their application in drug delivery system and biosensing platform. Pandey et al. have fabricated an electrochemical DNA biosensor with modified self assembly of cystine on Au surface for the detection of pathogenic bacterium *Escherichia coli* with the detection range of complementary DNA concentration from 1×10^{-6} M to 1×10^{-20} M at 25°C and stability of 4 months when stored at 4°C (Pandey et al. 2010). The use of L-cysteine (Cys) in the biosensor fabrication have been widely explored due to the presence of favourable multifunctional groups (–SH, –NH2, and –COO) which provide intimate interaction between metallic ions and biomolecules (Pandey et al. 2014a). The use of carbon nanomaterials (CNMs) especially

graphene oxide (GO) in conjugation with L-Cysteine has been receiving a great deal of attention owing to their exceptional properties when bound on the gold (Au) substrate in electrochemical biosensor. GO comprises of graphene with modified surface consisting of hydroxyl, carboxyl and epoxyl functional groups that provides excellent electrocatalytic properties and easily dispersable in the range of aqueous solvents (Tiwari et al. 2015). However, GO is known to have a hybrid structure comprising of a mixture of sp^2 and sp^3 hybridized carbon atoms. This higly disrupted sp^2 carbon lattice and presence of numerous oxygen containing functional groups render it to be an electrical insulator and hence it shows poor electrochemical activity when compared with rGO (Pumera 2010; Srivastava et al. 2013; Wang et al. 2009; Zhou et al. 2009). Thus in order to restore the conductivity and improved electrochemical behaviour, reduction of GO ino rGO is essential. rGO is an analog of graphene with some residual oxygen and structural defects. This is found to have remarkable properties which include high conductivity due to the presence of oxygen containing functional groups, large surface area and biocompatbility etc (Srivastava et al. 2013). Several reduction methods have been adopted for the reduction of GO to rGO which includes hydrothermal reduction, electrochemical reduction, chemical reduction using reducing agents such as oxalic acid, hydroquinone, L-ascorbic acid etc. These methods are highly toxic and non environment friendly thus not suitable for the fabrication of biosensing platform. In order to overcome this problem, green synthesis has been proposed for the reduction of GO to rGO have been developed which has removed the use of these chemical agents. The presence of sulphur group in L-Cysteine allows eco-friendly reduction of GO to rGO and this method of reduction is called as green synthesis. rGO provides several properties such as high thermal and mechanical stability, large surface area, multifunctional groups, biocompatibility and electron transfer rate that make them ideal candidate for biosensor fabrication.

CHAPTER-4

Materials and Methods

4. Materials and Methods

4.1 Chemicals and reagents

Graphite powder, sodium hydroxide (NaOH), L-cysteine (Cys), N-hydroxysuccinimide (NHS), N-ethyl-N-(3-dimethylaminopropyl carbodimide (EDC), ethanolamine, 0.2 M glycine and other reagents along with solvents have been procured from Sigma Aldrich (India). Cardiac troponin-I (cTnI) and mouse monoclonal anti-cardiac troponin I (anti-cTnI) antibody has been purchased from Sigma-Aldrich, India. 50 nm thick gold-coated BK-7 glass disks (24 millimetre diameter) were procured from Autolab, Netherlands. Phosphate buffer saline (PBS) solution of pH 7.4 has been prepared using milli-Q water and stored at 4°C. All other solutions were prepared in ultrapure water (milli-Q, Millipore, 18.2 ohm resistivity) throughout the experiments.

4.2 Characterization

The morphological investigation of the modified graphene Cys hierarchical structures has been carried out using transmission electron microscopy (TEM, Hitachi Model, H-800). The scanning electron microscopy (SEM) images of the rGO-Cys/Au and anti-cTnI/rGO-Cys/Au electrode have been examined using SEM. To investigate the formation of rGO-Cys and GO, Fourier transformed infrared spectroscopy (FT-IR) measurements were carried out using PerkinElmer spectrometer (Model Spectrum BX) at 25^{0}C. The formed rGO-Cys nanocomposite has been recorded via FT-IR spectra using KBr in the frequency region of $400cm^{-1}$- 4000 cm^{-1}. Contact angle (CA) measurements were conducted using Data Physics OCA15EC. Kinetic analysis and online monitoring of anti-cTnI/rGO-Cys/Au disk has been conducted on an Autolab KEI Twingle SPR instrument using the modified Au disk as substrate surface. Electrochemical characterization studies have been performed via

electrochemical impedance spectroscopy (EIS) and cyclic voltammetry (CV) techniques using the Autolab Potentiostat/Galvanostat electrochemical system (Metrohm Autolab, The Netherlands) attached with a three electrode cell filled with phosphate buffer (PBS) containing 5 mM $[Fe(CN)6]^{3-/4-}$.

4.2.1 Transmission electron microscopy

Transmission electron microscopy is a microscopic technique in which electron beam pass through an ultra-thin specimen for sample interaction. Tungsten filaments (100keV-1 MeV) are used to accelerate electrons onto a specimen (diameter <200nm) via condenser lens system. Electron beam and sample interaction results into the formation of image which is further focussed and magnified through an imaging device or CCD camera. This technique provides high resolution images than the conventional microscopy.

Figure 4.1 Transmission electron microscopy (TEM): Hitachi Model, H-800 TEM

The TEM comprises of: (1) two or three condenser lenses to focus the electron beam on the sample, (2) an objective lens to form the diffraction in the back focal plane and the image of the sample in the image plane, (3) all other intermediate lenses to magnify the image or the diffraction pattern on the screen. TEM is commonly operated in Bright Field (BF) imaging mode. In BF mode the contrast formed directly by the adsorption and occlusion of electrons in the sample. Sample regions with thickness or higher atomic number and the region with no sample will appear bright. Other than structural characterization of nanomaterials (NMs) TEM can also be used to determine NM's melting point. The melting points of NMs determine by the electron diffraction disappearance which result due to the heat up of the nano materials with electron beam. Besides this, TEM also be used to study the electrical and mechanical properties of nanotubes and nanowires.

4.2.2 Fourier transform infrared spectroscopy (FTIR)

FT-IR spectroscopy is an analytical technique that can be used for structural characterization of organic materials. It is a chemically specific analysis technique that can be used to identify chemical compounds and substituent groups. When quanta of infrared light interact with the molecule, it may absorb energy and vibrate faster. This phenomenon is the basis of FT-IR spectroscopy. Infrared absorption only occurs when infrared radiation interacts with a molecule undergoing a change in dipole, and when the incoming photon has sufficient energy for the transition to the next vibrational energy states. These infrared absorption bands identify specific molecular components and structures. In the FT-IR spectra, the appearance or non-appearance of central vibrational frequency and is very sensitive to the chemical environment, thus providing valuable information regarding the presence of certain functional groups in the specific sample for their further characterization. FT-IR spectrophotometer has a spectrum in range of 400-4000cm^{-1}.

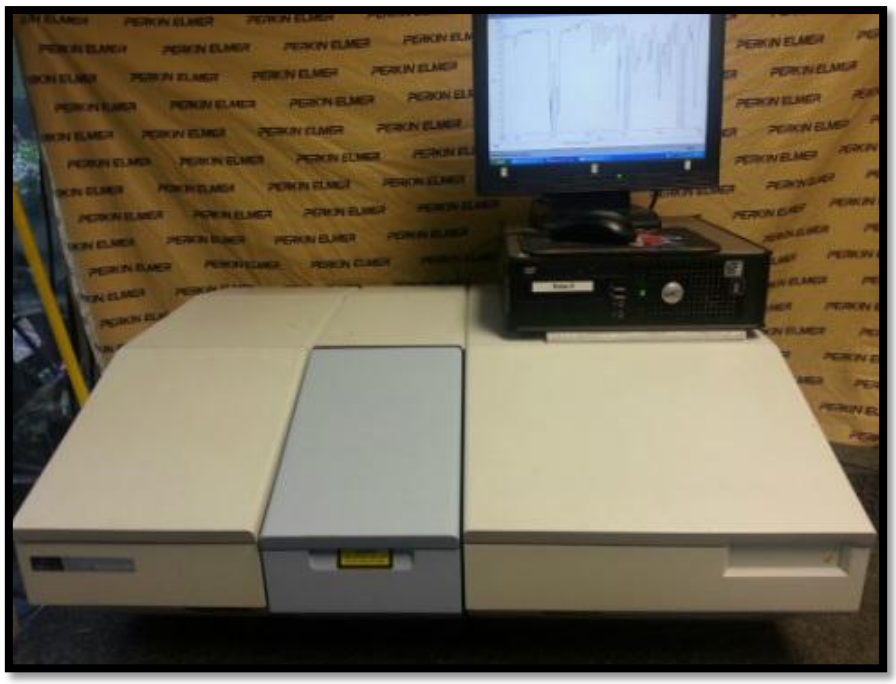

Figure 4.2 Fourier transform infrared spectroscopy (FT-IR) instrument: FT-IR spectrometer SPECTRUM BX II (PerkinElmer)

4.2.3 Contact angle (CA) measurements:

Contact angle (CA) is the angle at which a liquid/vapor interface meets a solid surface. The CA is specific for any given system and is determined by the interactions across interfaces. CA describes the shape of a liquid droplet resting on a solid surface. When a tangent line is drawn from a droplet to the touch of the solid surface, the angle between the tangent line and the solid surface is known as the contact angle. This technique is extremely surface sensitive, with the ability to detect properties of monolayers. Contact angle measurements were carried out to investigate the hydrophilic/hydrophobic character of the surface that can be co-related to SAM formation as well as the immobilization of enzyme onto the electrodes by sessile drop method. The Sessile drop method is an optical contact angle method. This method is used to estimate wetting properties of a localized region on a solid surface by measuring the angle between the baseline of the drop and the tangent at the drop boundary.

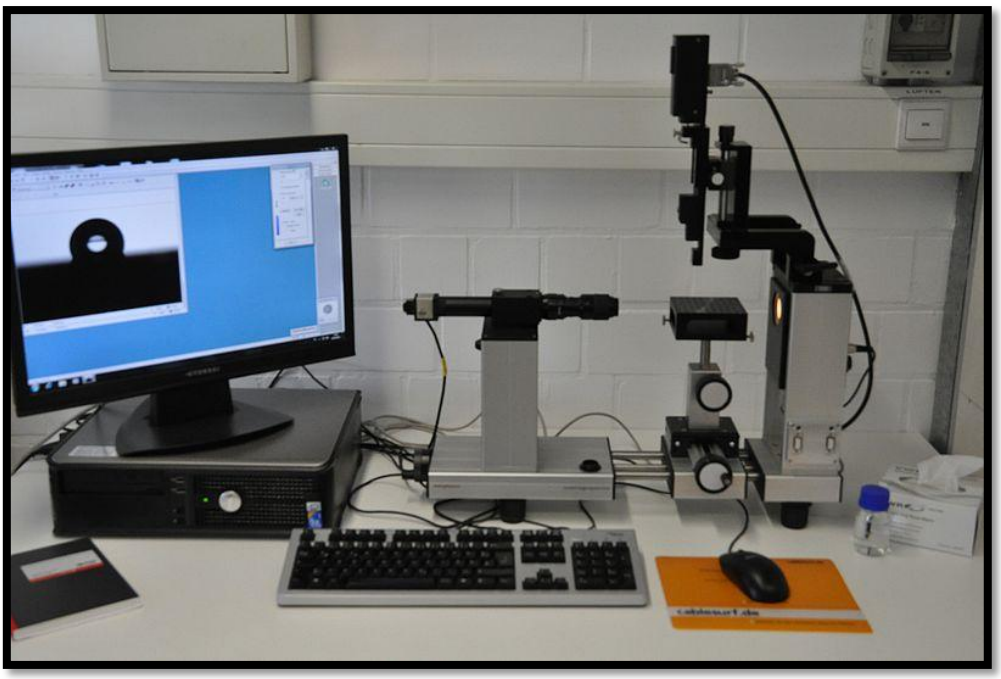

Figure 4.3 Optical Contact angle (OCA) instrument model of Data Physics; model number OCA15EC.

4.2.4 Cyclic voltammetry (CV):

Cyclic voltammetry is a type of potentiodynamic electrochemical measurement. To obtain a cyclic voltammogram, the voltage is varied in a solution and change in current is measured with respect to the change in voltage. It is a useful and versatile electroanalytical technique for studying the redox properties of electroactive species. In a CV experiment, the current increases as the potential reaches the oxidation potential of the analyte, whereafter it falls off as the concentration of the analyte is depleted close to the electrode surface. At this potential (often referred to as a switching potential), the direction of the potential scan is reversed, and the same potential window is scanned in the opposite direction (hence the term cyclic). As the applied potential is reversed, it will reach a potential where the reduction of product formed during forward scan starts producing a current of reverse polarity from the forward scan. This reduction peak will usually have a similar shape as that of an oxidation peak in other direction.

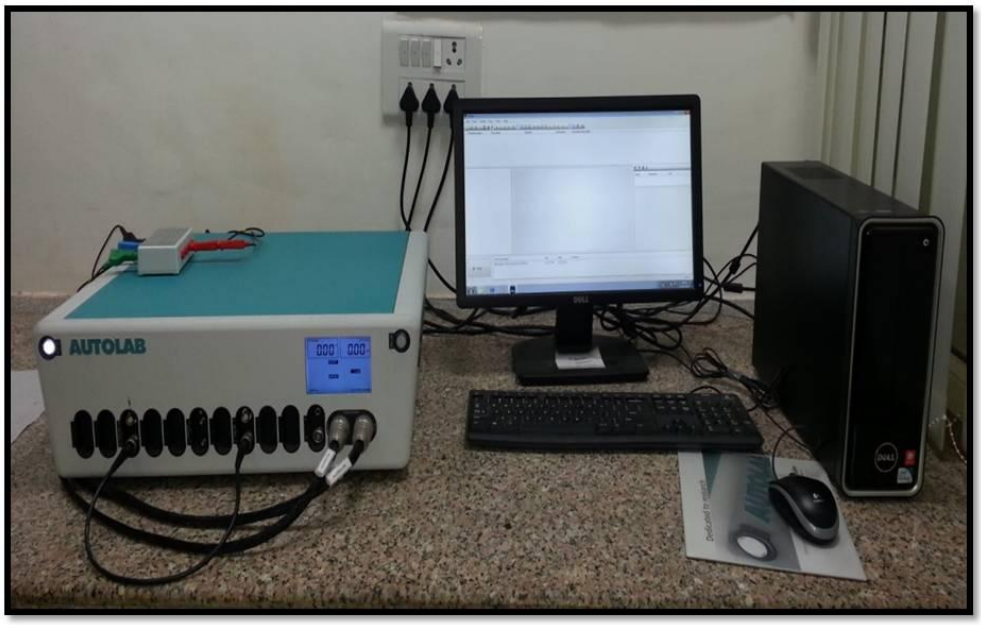

Figure 4.4 Potentiostat/Galvanostat instrument: Metrohm Autolab

4.2.5 Electrochemical impedance spectroscopy (EIS):

The electrochemical impedance spectroscopic (EIS) technique is used to study the resistive and capacitive behaviour at the interface of electrode surface and electrolyte in response to applied AC signal with varying frequency over a wide range (Orazem and Tribollet 2011; Srivastava et al. 2014). The resistance is given by Ohm's law: R = E/I, when DC signal is applied to an interface where, E and I are the applied voltage and resulting current, respectively. When an AC signal is applied to an interface, Ohm's law is again applicable, but the measured quantity is called the impedance Z and is given by Z = Ep / Ip, where Ep and Ip are the applied peak voltage and the measured peak current respectively. The AC impedance technique is commonly applied for the investigations of electrode kinetics and the reaction rates are related to the charge transfer resistances. EIS has wide range of advantages which include non-destructive behaviour and marked as an analytical technique which is highly sensitive to the bio-recognition events at the electrode/electrolyte interface (Ruan et al. 2002).

CHAPTER-5

Results and Discussion

5. Results and Discussion

5.1 Synthesis of graphene oxide

GO was synthesized using modified Hummer's method with slight modifications. Initially the pre-oxidized 1.5g natural graphite powder reacted with a mixture of 40 mL of 98% H_2SO_4, 5g $K_2S_2O_8$ and 5 g of P_2O_5 for 4h at 80°C. The obtained suspension was rinsed 4-5 times with deionized water (DW) and then dried under vacuum at 50°C. A mixture of chemicals including concentrated H_2SO_4: H_3PO_4 (180: 13) was added into the pre-oxidized graphite for further oxidization process with constant stirring for 5min. After this, 5gm of KMnO4 was added to the synthesized mixture and kept for stirring for 15 hrs at 50°C. On the completion of reaction time, the formed mixture was allowed to cool down at 25°C and then 200mL of ice cold water is added into the mixture followed by 1.5mL of 30% H_2O_2. The prepared powder was dispersed in distilled water ($0.1 mgmL^{-1}$) and kept under sonication for further study. Filteration of fine material from the synthesized mixture was performed by utilizing a U.S. standard testing sieve of pore size 30 µm. The obtained filtrate was centrifuged several times by DW, 30% HCl and ethanol (100mL of each) at 5000 rpm for about 3 h while the supernatant is discarded. The obtained sediment was suspended in 100mL of ether followed by filteration through a PTFE membrane with a pore size of 0.45 µm. Thus, the brown coloured graphene oxide (GO) powder was obtained when the semi solid material was vacuum dried for 12 h.

5.2 Green synthesis of rGO using GO wrapped cysteine microstructures

GO wrapped cys microstructures were synthesized by keeping 10mM L-cys solution under sonication for 5min. Later, the prepared $0.1 mgmL^{-1}$ GO dispersion was added to cys

solution. The solution was further sonicated till the solution colour turned into deep blue grey from brown colour. The growth process of rGO-Cys was observed for 6hrs (25^0C).

5.3 Self assembly of rGO-Cys nanocomposite on the gold surface

The hierarchical structures of rGO-Cys were self assembled onto the Au electrode (Figure 5.1). For the self assembly, the Au disk was dipped in the rGO-Cys solution overnight at room temperature. After this, the prepared electrode was rinsed with deionised water.

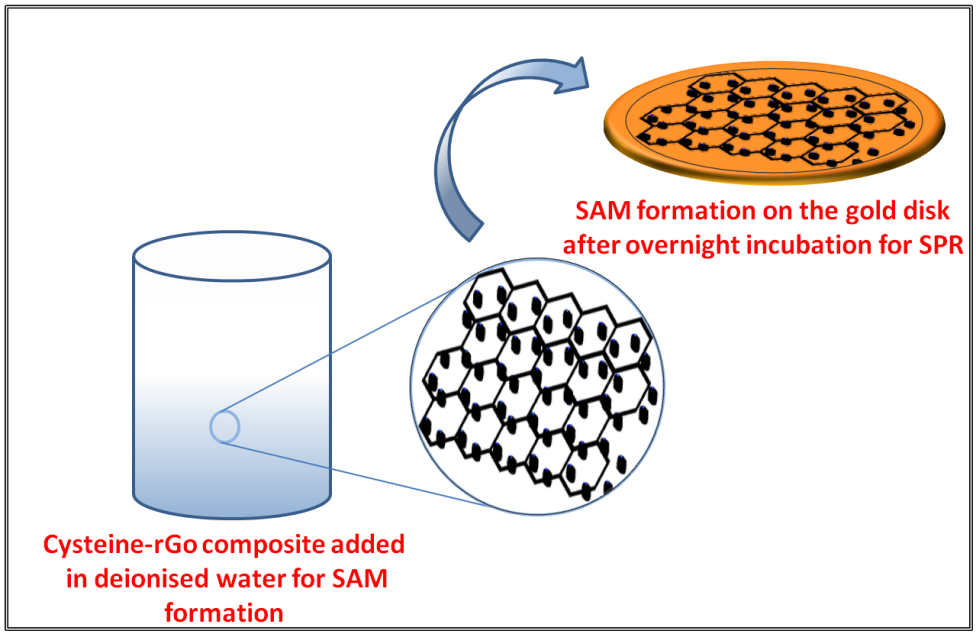

Figure 5.1 Schematic showing the synthesis of rGO wrapped cysteine self assembled monolayer (SAM).

Modified Au electrode was washed three times with ethanol in order to remove the bound cys molecules. Later, ethanol has been removed by washing of disk three times with demineralised water.

5.4 Biofunctionalization of the surface of rGO-Cys/Au disk with anti-cTnI

Figure 5.2 shows the Schematic configuration of the fabricated immunosensor. The process of immobilization of biomolecules on the rGO-Cys/Au electrode was done using SPR. The immobilization of monoclonal antibody of troponin I on the rGO-Cys/Au disk involved four step and all of them were monitored using SPR. Au electrode modified with rGO-Cys was docked into the instrument and later flushed with prepared PBS (pH 7.4) for 120 seconds to obtain a stable baseline. Then the modified Au surface was treated with a mixture of 0.4 M EDC and 0.1 M NHS in the ratio of 1:1 for 600 seconds at 25℃. After this 30µL of 10ugmL^{-1} anti-cTnI has been added onto the electrode surface to allow immobilization. In the next step 30uL of ethanolamine (pH 8) was added as a deactivation buffer for 300 seconds to remove excess of EDC/NHS molecule from the electrode surface. In the final step 30µL of 0.1mg/ml BSA was added onto the electrode in order to block the non-specific binding sites on the modified Au surface.

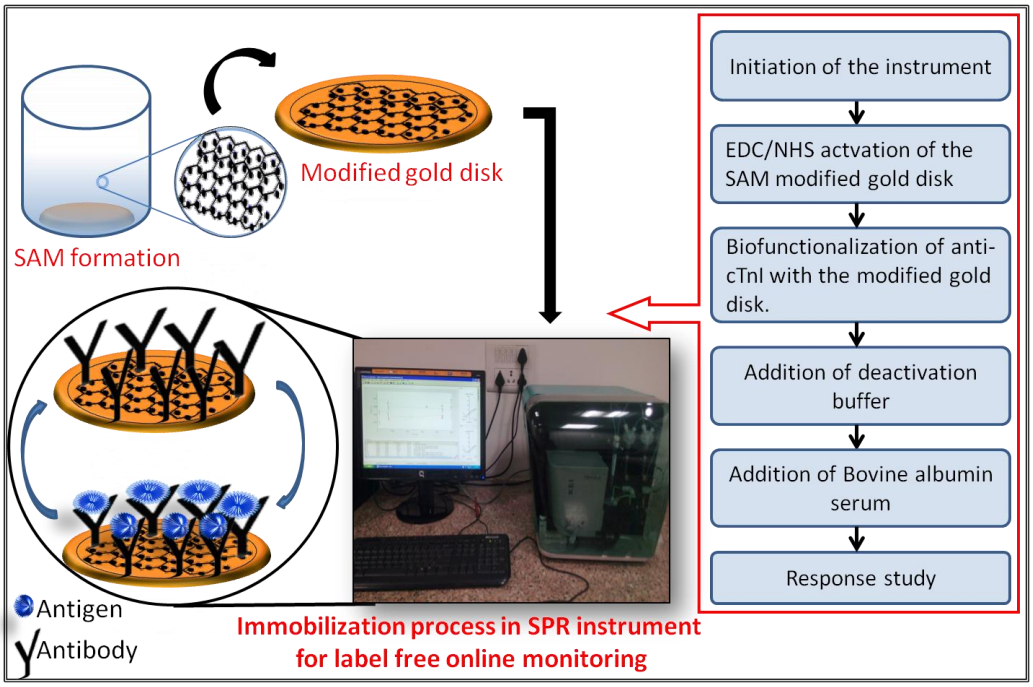

Figure 5.2 Schematic representation of the immobilization process of anti-cTnI onto modified SPR gold disk.

5.5 FT-IR studies

FT-IR spectroscopic studies were conducted to examine the formation of GO and rGO-Cys. It was observed that the FTIR spectra of GO showed characteristics peaks at 3461, 1630 cm^{-1} corresponds to O-H stretching, stretching vibration of C=O bonds of carboxylic acid group respectively, whereas the peak at 1384 cm^{-1} corresponding to the deformation of O-H. The peak seen at 1124 cm^{-1} corresponded to the presence of stretching vibration of epoxy C-O bonds. Whereas in case of rGO/Cys the presence of additional peaks at 1484 cm^{-1} is attributed to the stretching vibrations of alkane group while the peak at about 1191 cm^{-1} provides the evidence of secondary amide peaks indicating the presence of Cys on the GO sheets. (Figure 5.3)

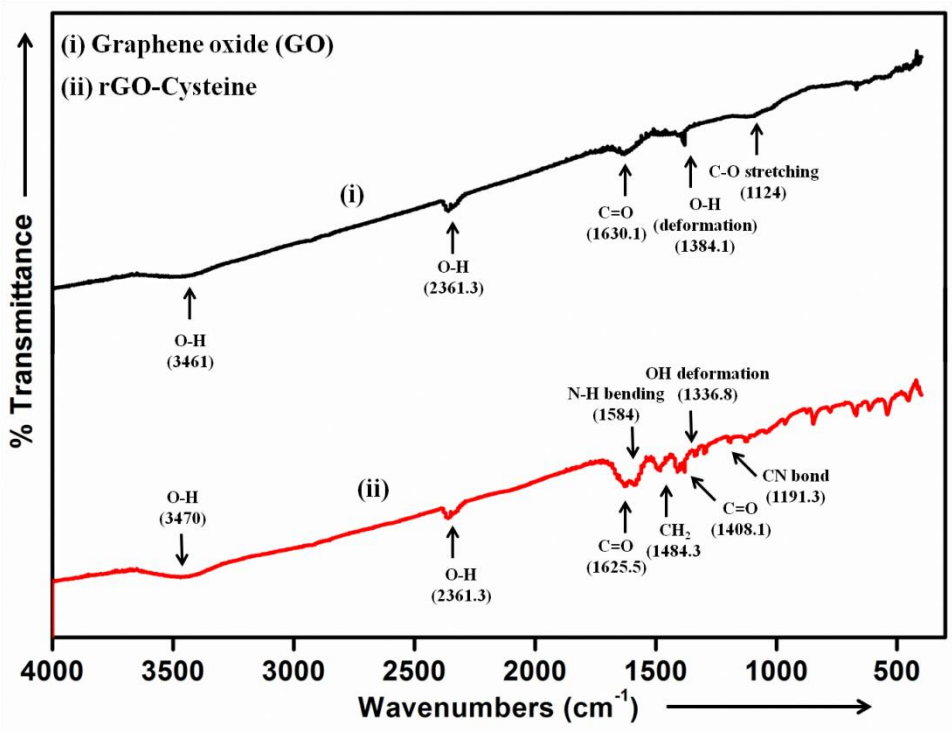

Figure 5.3 FTIR spectra of (i) GO and (ii) rGO- Cys nanocomposite.

5.6 Transmission electron microscopy studies

The TEM studies were performed to examine the size, shape and crystallanity of synthesized product The TEM images of GO sheets reveal a typical reppled and crumpled morphology (Figure 5.4(a)). The result shown in Figure 5.4(b), indicates that the formation of flower like structure of cys microstructures which is well covered by rGO.

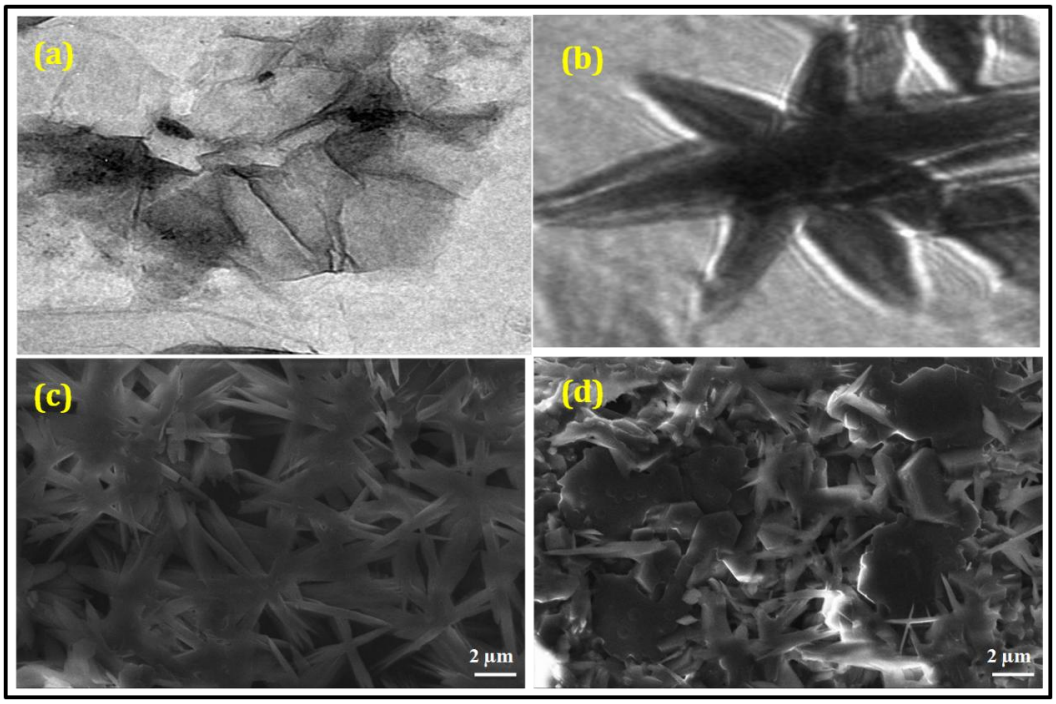

Figure 5.4 Transmission electron microscopic images of a) graphene oxide (GO) EM images. (b) rGO wrapped Cys (0.1M) (c) SEM image of rGO-Cys/Au electrode and (d) SEM image of anti-cTnI/rGO-Cys/Au electrode.

5.7 Scanning electron microscopy (SEM) studies

Scanning electron microscopic (SEM) images of the self assembly of rGO-cys at the Au electrode before and after immobilization of anti-cTnI has been shown in Figure 5.4(c) and (d). It has been observed that, before immobilization of anti-cTnI biomolecules, the electrode i.e. rGO-cys/Au appears as disordered semi flower like structure of cys formed under the rGO. Whereas after anti-cTnI immobilization the electrodes appears to have

homogenous surface coverage which is due to the covalent linking of the amino terminated antibodies with the carboxyl group of Cys.

5.8 Contact angle studies

To confirm the immobilization of anti-cTnI on the rGO-Cys surface, CA measurements were carried out using the sessile drop method. It was observed that the value of the CA decreased dramatically from 110.26^0 (bare Au) to 45.6° for rGO-Cys/Au electrode which indicated the formation of self assembly of rGO-Cys at the Au surface. After immobilization of the anti-cTnI, the value of contact angle further decreased to 18.4 showing the hydrophilic nature of the immobilized monoclonal antibody Figure 5.5(c). CA studies have been performed in triplicate sets by using different electrodes and the variation was observed within the range of ±3.

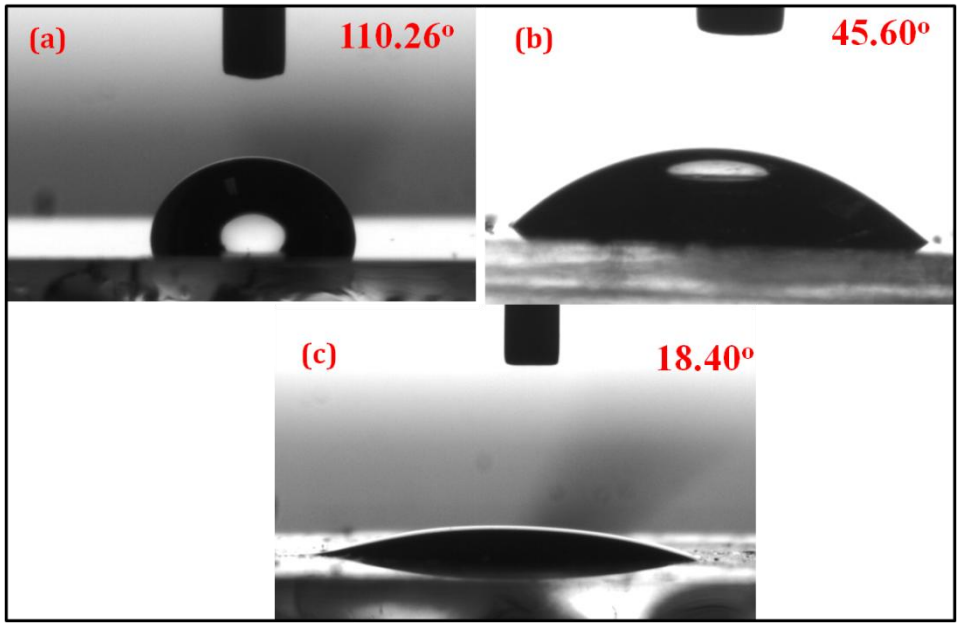

Figure 5.5 Contact angle analysis of a) Bare Au electrode; b) rGO-Cys/Au and c) anti-cTnI rGO-Cys/Au electrode.

5.9 Immobilization of monoclonal antibody on rGO-Cys/Au disk

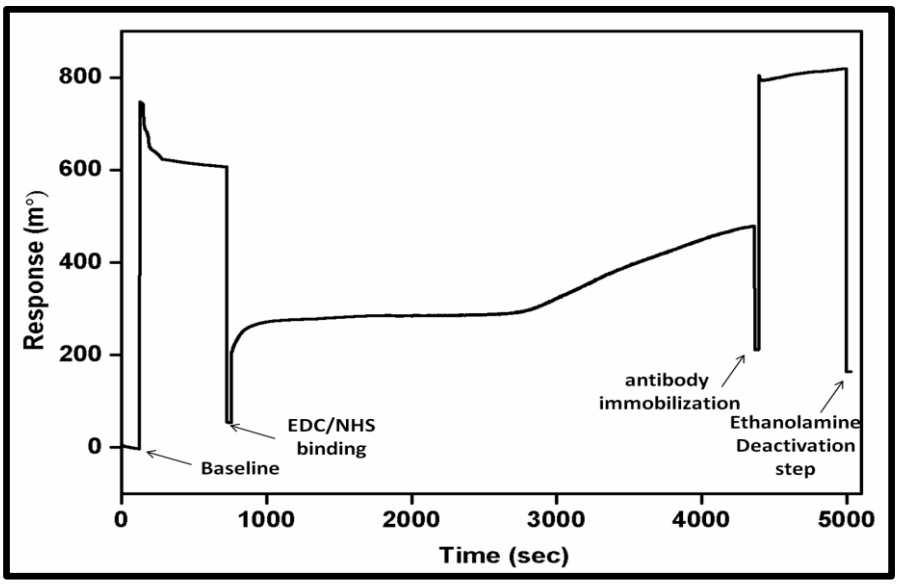

Figure 5.6 Graph showing the immobilization of anti-cTnI (10µgmL^{-1}) onto the modified SPR Au disk to fabricate BSA/anti-cTnI/rGO-Cys/Au electrode.

The functionalized disk was first docked to the KEI Twingle, Autolab instrument and primed with running buffer (PBS of pH 7.4) using a flow rate 50µL min^{-1} for 120s. This step was performed to stabilize the surface and to set the baseline (Zimple et al). After this step, 30µL of 10µg/mL anti-cTnI was added for the immobilization on rGO-Cys/Au disk using EDC/NHS chemistry through the flow channels of the sensor followed by washing with buffer (Figure 9). It was observed that a 14 min injection of the antibody was sufficient to achieve the signal with concentration of 10µgmL^{-1} antibody after that the response gets saturated. The increase in SPR angle with time clearly indicated gradual binding of the anti-cTnI on the rGO-Cys/Au disk. The observed difference in SPR angle (160millidegrees) before and after the bio-functionalization of anti-cardiac troponin I corresponds to 1.3 ng/mm^2 of anti-cTnI (Change in 120 millidegrees is equal to 1ng/mm^2 of surface change which indicate molecular binding) on rGO-Cys/Au disk (S. K. Arya et al). This result indicates that 11.7ng of anti-cTnI is immobilized over an area of 9 mm^2 on rGO-Cys/Au disk.

Further ethanolamine (pH 8) can be used to remove the unbound EDC/NHS molecules from the modified surface of sensor.

The concentration of the anti-cTnI used during the experiment was also optimized. Various concentration of detection antibody in the range of 1-10μg mL^{-1} was added on Cys-rGO/Au disk upto the level when the saturation in response angle has been achieved. The obtained results show that at a concentration of 10μg mL^{-1} of anti-cTnI, the higher signal was obtained and on further increasing the concentration there was no change in the signal. The test was also performed with higher concentrations of anti-cTnI but did not get considerable responses.

5.10 Response studies

The SPR signal obtained with different concentration of cTnI (1-20ngmL^{-1}) is shown in Figure 5.7. The graph for response angle versus time plot clearly indicates that the response angle is increasing with the increase of cardiac troponin I concentration confirming the binding of cTnI with the sensor platform. (association phase).Immediately after the completion of association phase, the remaining analyte on the surface of Au disk is washed away through the flow channels by utilizing the running buffer. This resulted in the dissociation phase indicated by the sharp dip in the SPR signal representing the changes in bulk refractive index (Arya et al. 2006). Similar conditions were maintained before and after association phase so the difference between the SPR signals suggests the amount of bound cTnI biomolecules with the anti-cTnI covalently bound on rGO-Cys/Au disk.

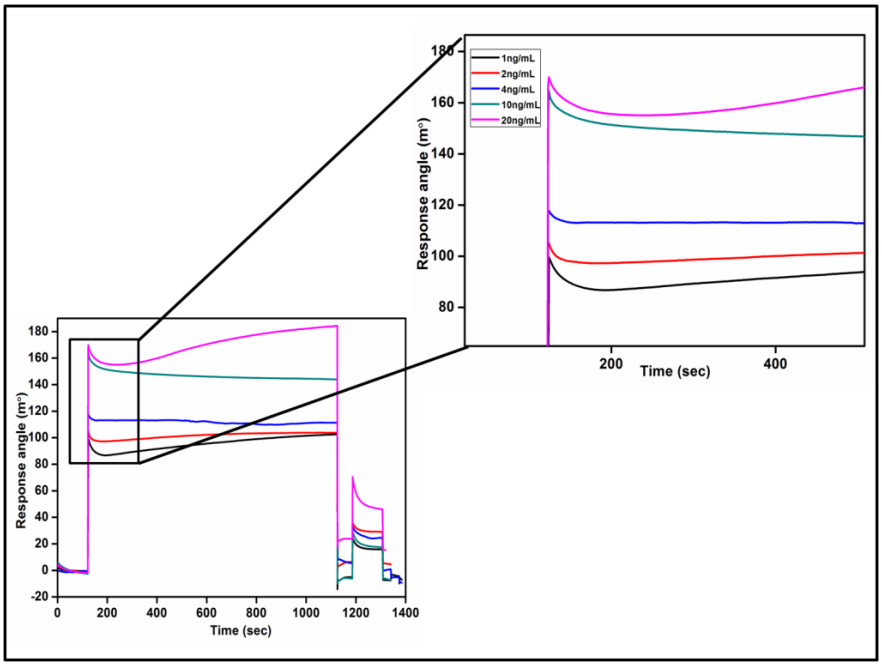

Figure 5.7 Sensogram showing response of immunosensor BSA/anti-cTnI/rGO-Cys/Au in successive injections of cTnI concentrations (1ngmL-20ngmL).

Next step marked the regeneration phase which reactivates the catalytic binding site and also works to remove the remaining bound substrate. In this step regeneration buffer was added which ultimately bring back the SPR signal to the baseline. Control experiment was conducted parallely to the working experiment under same conditions with the difference of adding running buffer instead of cTnI biomolecules during association phase and marked by straight line representing no binding during SPR studies.

The overall experiment was performed in triplicate and found to be almost having similar response with the error rate of within 5%. For quantification the graph of shift in SPR angle was plotted as a function of cTnI concentration and a straight line was obtained showing the linearity in the range of 1-20ngmL^{-1} of cTnI (Figure 5.8). Kinetic data obtained while monitoring the molecular events have been shown in the Table 5.1.

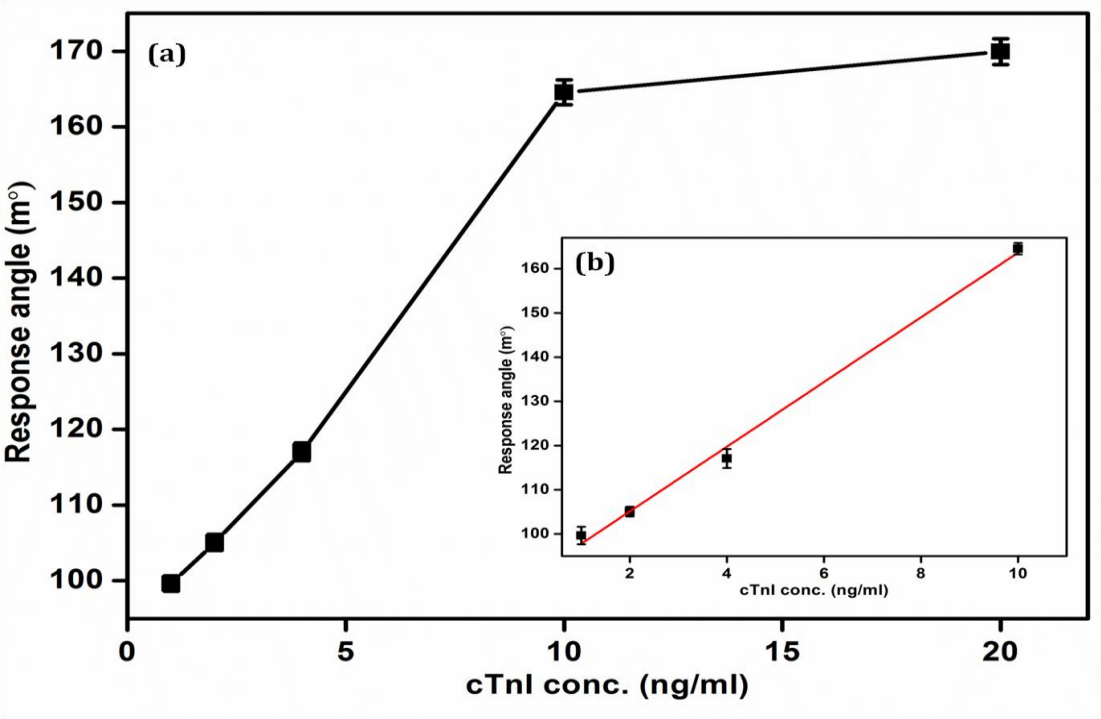

Figure 5.8 (a) Calibration plot showing the variation of change in response angle with increasing concentrations of cTnI; Inset b figure shows linear fit of change in response angle versus cTnI concentrations.

Conc. (ng/ml)	Surface density	Amount	No. of bound molecules
1	0.0381	0.3010	7.55×10^{9}
2	0.0621	0.4906	1.23×10^{10}
4	0.1545	1.2206	3.062×10^{10}
6	0.1565	1.2364	3.102×10^{10}
10	0.2360	1.8644	4.678×10^{10}

Table 5.1 Kinetic Data showing molecular binding events on rGO-Cys/Au as a function of increasing cTnI concentration through SPR technique.

5.11 Electrochemical characterization:

The cyclic voltammetric (CV) studies were performed on the rGO-Cys/Au and BSA/anti-cTnI/rGO-Cys/Au bio-electrodes as a function of scan rate in the range of 10-250mV/sec (Figure 5.9 and 5.10). The separation between the peaks of both the electrodes increases and shifts toward the higher potential side with increasing scan rate leading to diffusion controlled (quasi reversible) process.

The plot between the anodic and cathodic peak current versus square root of scan rate has been shown in the Inset (a) of Figure 5.9 and 5.10. The linear curve fitting follows the following equations:

$$\mathbf{I_{pa}}_{(rGo\text{-}Cys/Au)} = [0.03373\ mA(s/mV) \times (scan\ rate[mV/s])^{1/2}] + 0.0403mA$$

$$R^2 = 0.98385 – (Eq.\ 5.1)$$

$$\mathbf{I_{pa}}_{(rGo\text{-}Cys/Au)} = -[0.0154\ mA(s/mV) \times (scan\ rate[mV/s])^{1/2}] – 0.0852mA$$

$$R^2 = 0.97283..... (Eq.\ 5.2)$$

$$\mathbf{I_{pa}}_{(BSA/anti\text{-}cTnI/rGo\text{-}Cys/Au)} = [0.02426\ mA(s/mV) \times (scan\ rate\ [mV/s])^{1/2}] + 0.03581mA$$

$$R^2 = 0.94011 ….. (Eq.\ 5.3)$$

$$\mathbf{I_{pa}}_{(BSA/anti\text{-}cTnI/rGo\text{-}Cys/Au)} = -[0.01118\ mA(s/mV) \times (scan\ rate[mV/s])^{1/2}] – 0.13811mA$$

$$R^2 = 0.99976 …... (Eq.\ 5.4)$$

The plot between the potential peak shift ($\Delta V = V_{pa} – V_{pc}$, V_{pa}) is anodic peak potential and V_{pc} is cathodic peak potential) and the square root of the scan rate obtained for rGO-Cys/Au

electrode and BSA/anti-cTnI/rGO-Cys/Au have been shown in the Inset (b) of figure 7 and 8 respectively. The following linear equations were obtained-

$\mathbf{I_{pa}}$ $_{(rGo\text{-}Cys/Au)}$ = [0.049 V(s/mV) x (scan rate[mV/s])$^{1/2}$] + 0.125V

R^2= 0.98182 ….. (Eq. 5.5)

$\mathbf{I_{pa}}$ $_{(BSA/anti\text{-}cTnI/rGo\text{-}Cys/Au)}$ = [0.03544 V(s/mV) x (scan rate [mV/s])$^{1/2}$] + 0.17391V

R^2= 0.99296 …..(Eq. 5.6)

The linear relationship obtained in these equations indicates the electrochemical reaction taking place are diffusion controlled (quasi-reversible). The diffusion coefficient of the redox species {$[Fe(CN)_6]^{3-/4-}$ has been estimated using Randel-Sevcik equation.

$$I_p = (2.69 \text{ X } 10^5)\, n^{3/2}\, AD^{1/2}\, Cv^{1/2} \quad \text{……. (Eq. 5.7)}$$

Where I_p is the peak current of the bio-electrode, n is the number of electrons transferred (1), A is surface area of the electrode (0.25 cm^2), D is diffusion coefficient C is the concentration of redox species (5 X 10^{-3} mol cm^{-2}) and v is the scan rate (50 mV s^{-1}). The diffusion coefficient has been obtained as 2.901 X 10^{-6} cm^2 s^{-1}. Further, the surface concentration of BSA/anti-cTnI/rGO-Cys/Au bio-electrode has been calculated through Brown-Anston Model as given in equation (5.7):

$$Ip = n^2 F^2 \gamma A v (4RT)^{-1} \quad \text{…… (Eq. 5.8)}$$

Where Ip represents the peak current, A is the surface area of electrode, v is the scan rate (V/s). γ is the surface concentration of the adsorbed electro-active species, F is the faraday constant (96485 $Cmol^{-1}$), R is the gas constant (8.314 J $mol^{-1}K^{-1}$) and T is the room

temperature (25°C or 298K). The surface concentration of BSA/anti-cTnI/rGO-Cys/Au is estimated to be as 2.398 X 10^{-8} mol cm^{-2}.

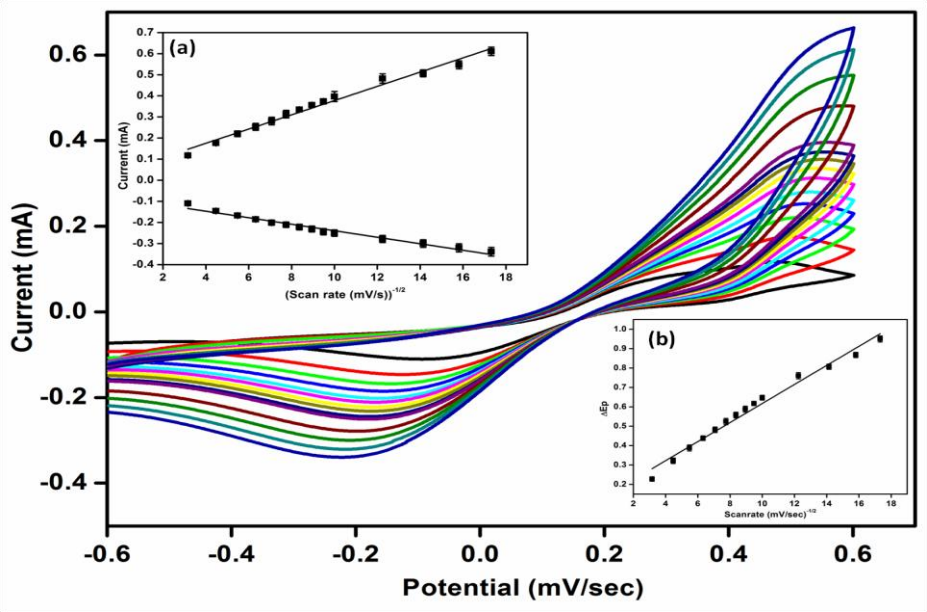

Figure 5.9 Cyclic voltammogram (CV) studies of rGO-Cys/Au electrode as a function of scan rate (10-250 mV/s), Inset (a) shows the magnitude of oxidation and reduction current generated as response of scan rate (mV/sec), Inset (b) shows the potential as function of scan rate.

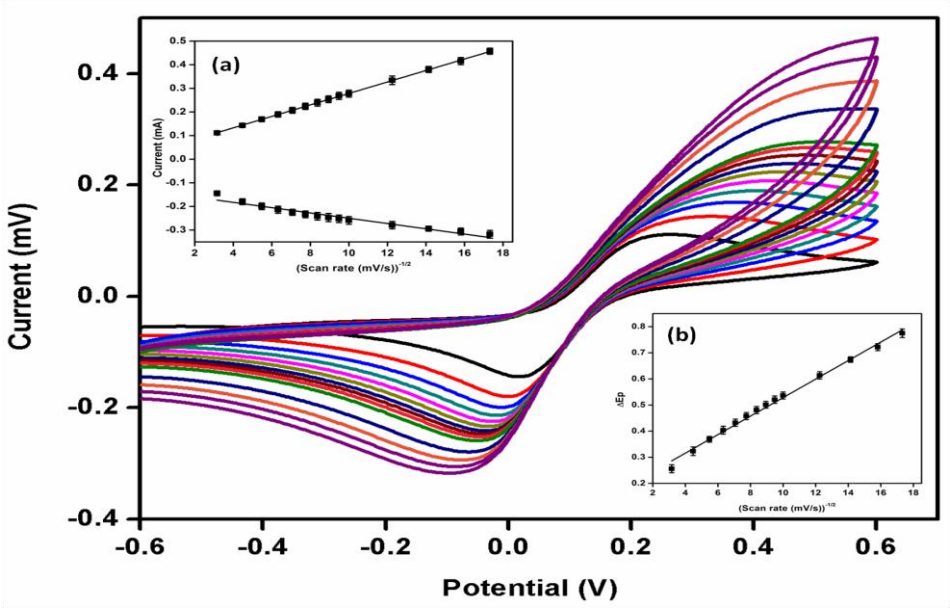

Figure 5.10 CV studies of BSA/anti-cTnI/rGO-Cys/Au bio-electrode as a function of scan rate (10-300 mV/s), Inset (a) shows the magnitude of oxidation and reduction current generated as response of scan rate (mV/sec), Inset (b)shows the potential as function of scan rate.

5.12 Electrochemical Response Studies:

Electrochemical impedance spectroscopy (EIS) is a powerful tool for the study of interfacial charge transfer processes occurring at the interfaces of the electrode surface and electro-active substances. In the electrochemical impedance spectra, the Nyquist plot shows a semicircle which represents the electron transfer resistance process (Rct) and the value of Rct usually depends on the dielectric and insulating properties at the electrode–electrolyte interface. The observed analytical signal (Rct) in Figure 5.11 shows linear relationship with cTnI bio-molecules ranging from concentration 1 to 80ngmL^{-1} and the linear equation for BSA/anti-cTnI/rGO-Cys/Au electrode was calculated and is given by the following equation:

Rct (Ω) = 2.865 + 0.016 (Ω mL ng^{-1}) x conc. of cTnI (ngmL^{-1}) .....(Eq 5.9)

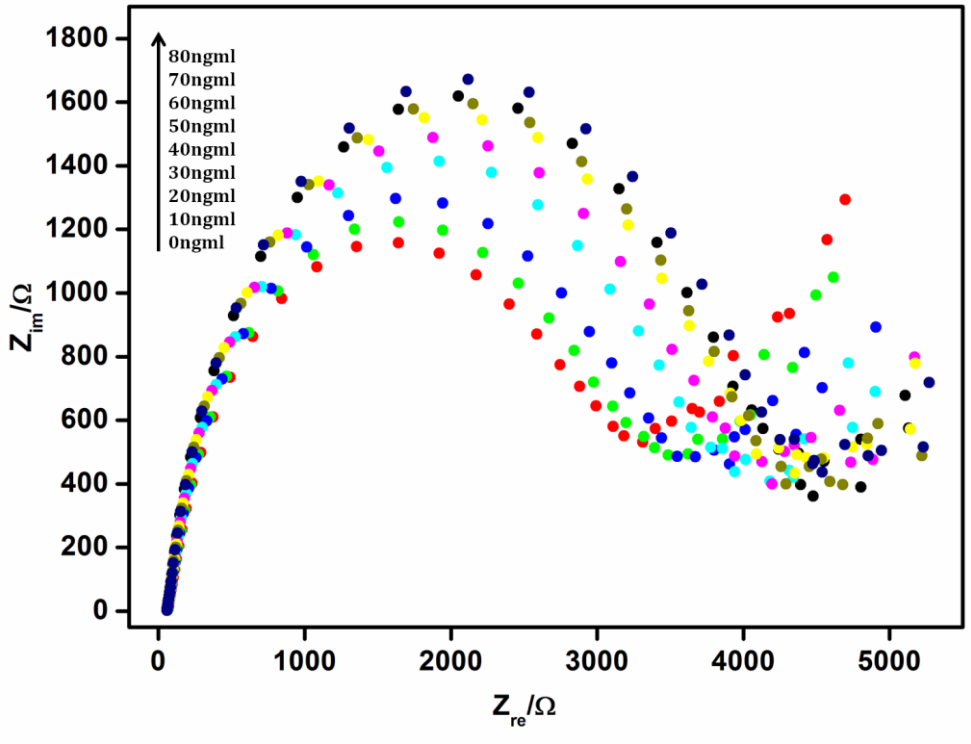

Figure 5.11 EIS response plot of BSA/anti-cTnI/rGO-Cys/Au electrode as a function of cTnI concentration (1-80ngmL^{-1}) in 5 mM $[Fe(CN)_6]^{3-/4-}$ PBS solution at pH 7.4.

The value of linear regression coefficient is found to be 0.9956. The lower detection limit (LDL) has been calculated using the expression 3σ/m for the linear region is found to be 0.0697 $ngml^{-1}$, where σ is the standard deviation of the blank (rGO-Cys/Au electrode) and m is the slope of the calibration curve. The sensitivity of the fabricated electrode was found to be 0.06428Ω ng^{-1} $mLcm^{-2}$. For comparison, the sensing properties of rGO-Cys/Au electrode via SPR techniques have also been performed. The sensing experiment was repeated thrice and the imprecision of the data was found to be within 5% as indicated by the error bars (Figure 5.12). The performance of EIS detection indicates that the enhanced electron transfer rate was due to the rGO-Cys and it may perhaps due to the highly specific antigen-antibody immune reaction.

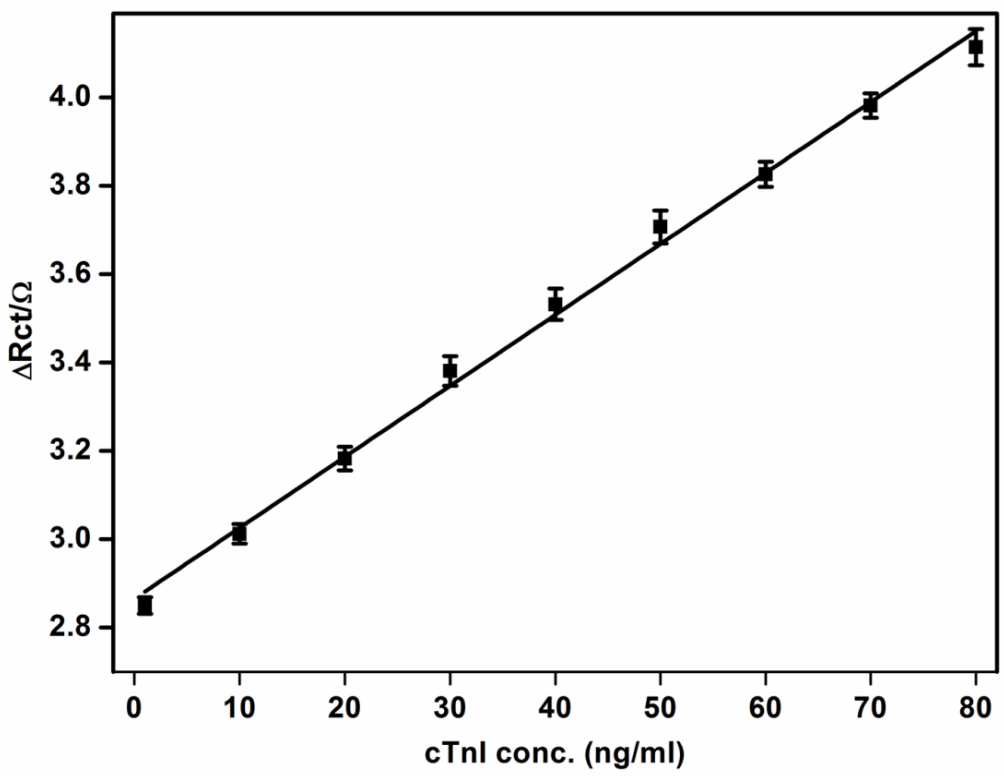

Figure 5.12 EIS linearity plot showing the response of BSA/anti-cTnI/rGO-Cys/Au electrode with increasing concentration of cTnI ranging from 1-80 $ngmL^{-1}$ in PBS solution (pH 7.4) containing 5mM $[Fe(CN)_6]^{3-/4-}$.

The biosensing sensing performance of the fabricated BSA/anti-cTnI/rGO-Cys/Au electrode based biosensor has been compared with other biosensors published in literature for cTnI detection (Table 5.2). In this context, (Wei et al. 2003) have fabricated an optical immunosensor for monitoring the concentration of cTnI in blood serum via sandwich assay by using avidin as an intermediate layer and biotinylated-2F11 as the capturing antibody. The fabricated immunosensor showed sensitivity with the detection range from 0.5 to 20 μg L^{-1} while in the present work the detection range of fabricated immunosensor is from 1ngmL^{-1} to 80ngmL^{-1}. MCM-41 mesoporous material modified carbon paste electrode (MCM-MCPE) have been fabricated by Guo et al. with the detection limit of 0.5 ngmL^{-1} (Guo et al. 2005) while in the present work the fabricated bio-electrode shows the limit of detection of 0.069 ngmL^{-1}.

Techniques Involved	Electrode material	Detection limit ($ngmL^{-1}$)	Linearity ($ngmL^{-1}$)	label/unlabel	Reference
Anodic stripping voltammetry	MCM-41 mesoporus material	0.5	0.8-5.0	Labelled	*(Guo et al. 2005)*
Electrochemical immunoassay	Silver enhancement on gold nanoparticles	0.8	1-20		(Chu et al. 2005)
Guided mode resonance biosensor	GMR filter chips	0.05	0.05-10	Label free	*(Kim et al. 2010)*
Optomagnetic technology via sandwich immunoassay	Supermagnetic nanoparticles	0.03	0.03-6.5	Labelled	*(Dittmer et al. 2010)*
Field effective transistor (FET)	Silicon oxide nanowire	2	----	Label free	*(Cheng et al. 2011)*
FET	Silicon	0.092	0.092-46	Label free	*(Kong et al. 2012)*
Nanoelectrode arrays	Carbon nanofiber	0.2	----	Label free	(Periyakaruppan et al. 2013)
Photonic crystal biosensor	PC-TIR biosensor	0.1	----	Label free	*(Zhang et al. 2014)*
Frequency response Analysis (FRA)	rGO-Cys/Au	0.0697	1-80	Label free	This work

Table 5.2 Comparison of the present work with previously reported cTnI biosensors.

5.13 Calculation of Association constant between the covalently bound anti-cTnI and cTnI

The Lagmuir isotherm approach has been used to determine the association constant (Ka) for binding interaction which assumes that the binding energy is equal for all the available binding sites. The value of Ka has been estimated by relating the change in Rct value with the binding of cTnI biomolecule on anti-cTnI/rGO-Cys/Au. The obtained curve is represented by the following equation,

$$M = 1 - \frac{\Delta Rct(co)}{\Delta Rct(ci)}$$

……Eq 5.10

where M is the number of occupied binding sites, Rct (co) is charge transfer resistance without cTnI, and Rct (ci) indicate charge transfer resistance with desired concentration of anti-cTnI.

According to the Langmuir isotherm, M can be related to the association constant by utilizing the equation as follows:

$$M = \frac{K_a\, C}{1 + K_a\, C}$$

……Eq. 5.11

where Ka, c indicates the association constant and the molecular concentration in the solution.

From equation (5.10) and (5.11), we have

$$K_a\, C = \frac{Rct(ci) - Rct(co)}{Rct(co)} = \frac{\Delta Rct}{Rct(co)}$$

.....Eq.5.12

Figure 5.13 shows the curve plotted by using equation 5.12 between ΔRct /Rct(co) and the concentration of cTnI. This indicates that the ΔRct /Rct(co) varies linearly with the cTnI concentration and represented by the following equation,

$$\Delta\, Rct/Rct(co) = 0.01 + 0.005\ (\Omega\ mL\ ng^{-1}\ cm^{-2}) \times conc.\ of\ cTnI\ (ngmL^{-1})$$ .....Eq 5.13

with a correlation coefficient of 0.993.

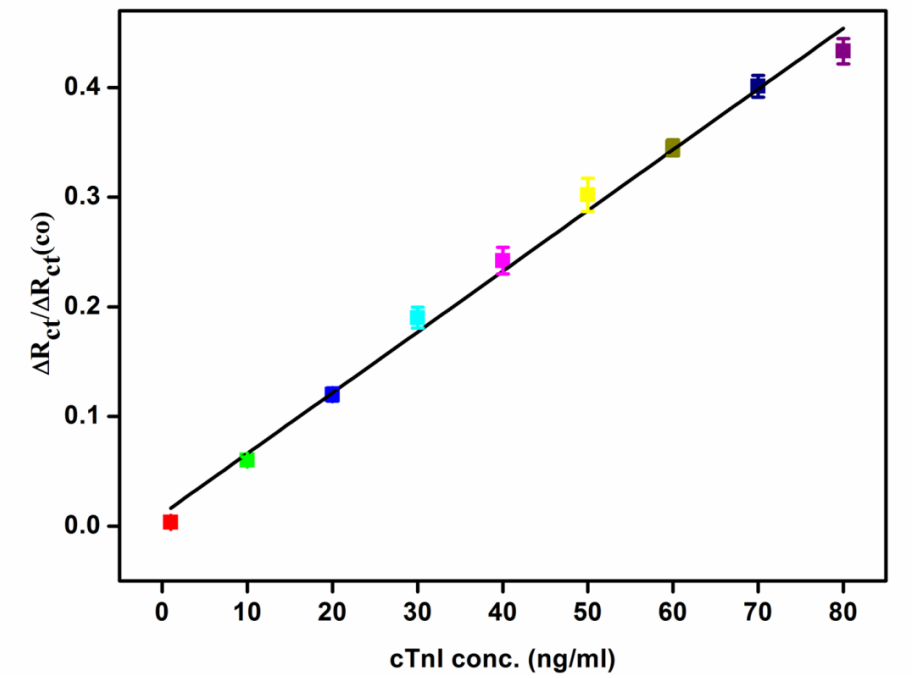

Figure 5.13 Graph between ΔRct/Rct(co) and the concentration of cTnI for calculating association constant (Ka) of anti-cTnI/rGO-Cys/Au electrode.

CHAPTER-6

Conclusions

6. Conclusions

We have fabricated the SPR biosensor based on self assembly of rGO-Cys nanocomposite for the detection of cTnI biomarker. The graphene oxide wrapped cysteine has been synthesized at micro-scale level and self assembled on Au coated glass substrate. The morphological and structural studies show that the synthesized composite have certain morphology and is evenly self assembled on the Au electrode. Using the SPR technique with appropriate optimized protocol, monoclonal antibody has been immobilized on the rGO-Cys/Au electrode with online monitoring of biomolecular interactions. It was observed that 11.7ng of anti-cTnI was successfully immobilized on the electrode surface. Kinetic analysis of biomolecular binding events on rGO-Cys/Au as a function of increasing cTnI concentration using SPR reveals that the surface density has been increased from 0.0381 to 0.23, number of bound biomolecules increased from 7.5×10^{9} to 4.6×10^{10}. Sensing results carried out using electrochemical impedance spectroscopy shows that the cardiac troponin I can be detected by the fabricated biosensor in the range of 1-80 $ngmL^{-1}$. This fabricated biosensor is having efficient detection range, lower detection limit and showed high sensitivity as well. Further, research is in progress to validate the fabricated biosensor by evaluating its performance against blood serum sample.

CHAPTER-7

Future Perspectives

7. Future Perspectives

The present experimental investigations conducted on graphene wrapped cysteine self assembly has implications towards point-of-care diagnostics. This is attributed to the fascinating properties of this composite. It would be interesting to incorporate metal oxides into graphene wrapped cysteine self assembly to further enhance the biosensing properties. In addition to this, the use of SPR technique would eventually lead to a new class of biosensors with a variety of applications in clinical diagnostics. SPR technique can further be utilized to analyse the adsorption process through Langmuir adsorption isotherm and Freundlich adsorption isotherm to appropriately describe the biomolecular interactions. These techniques provide a path breaking potential for the development of label free biosensors to diagnose cancer as well.

CHAPTER-8

References

8. References

Ahammad, A.S., Choi, Y.-H., Koh, K., Kim, J.-H., Lee, J.-J., Lee, M., 2011. Electrochemical detection of cardiac biomarker troponin I at gold nanoparticle-modified ITO electrode by using open circuit potential. Int. J. Electrochem. Sci 6(6), 1906-1916.

Arya, S.K., Solanki, P.R., Singh, R.P., Pandey, M.K., Datta, M., Malhotra, B.D., 2006. Application of octadecanethiol self-assembled monolayer to cholesterol biosensor based on surface plasmon resonance technique. Talanta 69(4), 918-926.

Campuzano, S., Gálvez, R.o., Pedrero, M.a., de Villena, F.J.M., Pingarrón, J.M., 2002. Preparation, characterization and application of alkanethiol self-assembled monolayers modified with tetrathiafulvalene and glucose oxidase at a gold disk electrode. Journal of Electroanalytical Chemistry 526(1), 92-100.

Cheng, Y., Chen, K.-S., Meyer, N.L., Yuan, J., Hirst, L.S., Chase, P.B., Xiong, P., 2011. Functionalized SnO 2 nanobelt field-effect transistor sensors for label-free detection of cardiac troponin. Biosensors and Bioelectronics 26(11), 4538-4544.

Chu, X., Fu, X., Chen, K., Shen, G.-L., Yu, R.-Q., 2005. An electrochemical stripping metalloimmunoassay based on silver-enhanced gold nanoparticle label. Biosensors and Bioelectronics 20(9), 1805-1812.

Chu, X., Lin, Z.-H., Shen, G.-L., Yu, R.-Q., 1995. Piezoelectric immunosensor for the detection of immunoglobulin M. Analyst 120(12), 2829-2832.

Daghestani, H.N., Day, B.W., 2010. Theory and applications of surface plasmon resonance, resonant mirror, resonant waveguide grating, and dual polarization interferometry biosensors. Sensors 10(11), 9630-9646.

Dittmer, W.U., Evers, T.H., Hardeman, W.M., Huijnen, W., Kamps, R., de Kievit, P., Neijzen, J.H., Nieuwenhuis, J.H., Sijbers, M.J., Dekkers, D.W., 2010. Rapid, high sensitivity, point-of-care test for cardiac troponin based on optomagnetic biosensor. Clinica Chimica Acta 411(11), 868-873.

E, K., 1971. Determination of optical constants of metals by excitation of surface plasmons. Zeitschrift Fur Physik 241(4), 313-&.

Fan, C., Plaxco, K.W., Heeger, A.J., 2003. Electrochemical interrogation of conformational changes as a reagentless method for the sequence-specific detection of DNA. Proceedings of the National Academy of Sciences 100(16), 9134-9137.

Fathil, M., Arshad, M.M., Gopinath, S.C., Hashim, U., Adzhri, R., Ayub, R., Ruslinda, A., Azman, A., Zaki, M., Tang, T.-H., 2015. Diagnostics on acute myocardial infarction: Cardiac troponin biomarkers. Biosensors and Bioelectronics 70, 209-220.

Frederix, F., Bonroy, K., Laureyn, W., Reekmans, G., Campitelli, A., Dehaen, W., Maes, G., 2003. Enhanced performance of an affinity biosensor interface based on mixed self-assembled monolayers of thiols on gold. Langmuir 19(10), 4351-4357.

Gauglitz, G., 1996. Opto-Chemical and Opto-Immuno Sensors. Sensors update 1(1), 1-48.
Ghindilis, A.L., Atanasov, P., Wilkins, M., Wilkins, E., 1998. Immunosensors: electrochemical sensing and other engineering approaches. Biosensors and Bioelectronics 13(1), 113-131.

Gu, J., Lu, X., Ju, H., 2002. DNA sensor for recognition of native yeast DNA sequence with methylene blue as an electrochemical hybridization indicator. Electroanalysis 14(13), 949.

Guo, H., He, N., Ge, S., Yang, D., Zhang, J., 2005. MCM-41 mesoporous material modified carbon paste electrode for the determination of cardiac troponin I by anodic stripping voltammetry. Talanta 68(1), 61-66.

Homola, J., 2003. Present and future of surface plasmon resonance biosensors. Analytical and bioanalytical chemistry 377(3), 528-539.

Jagadeesan, K.K., Kumar, S., Sumana, G., 2012. Application of conducting paper for selective detection of troponin. Electrochemistry Communications 20, 71-74.

Jung, L.S., Nelson, K.E., Stayton, P., Campbell, C.T., 2000. Binding and dissociation kinetics of wild-type and mutant streptavidins on mixed biotin-containing alkylthiolate monolayers. Langmuir 16(24), 9421-9432.

Karlsson, R., Fält, A., 1997. Experimental design for kinetic analysis of protein-protein interactions with surface plasmon resonance biosensors. Journal of immunological methods 200(1), 121-133.

Kim, W.-J., Kim, B.K., Kim, A., Huh, C., Ah, C.S., Kim, K.-H., Hong, J., Park, S.H., Song, S., Song, J., 2010. Response to cardiac markers in human serum analyzed by guided-mode resonance biosensor. Analytical Chemistry 82(23), 9686-9693.

Kong, T., Su, R., Zhang, B., Zhang, Q., Cheng, G., 2012. CMOS-compatible, label-free silicon-nanowire biosensors to detect cardiac troponin I for acute myocardial infarction diagnosis. Biosensors and Bioelectronics 34(1), 267-272.

Kumar, S., Kumar, S., Tiwari, S., Srivastava, S., Srivastava, M., Yadav, B.K., Kumar, S., Tran, T.T., Dewan, A.K., Mulchandani, A., 2015. Biofunctionalized nanostructured zirconia for biomedical application: a smart approach for oral cancer detection. Advanced Science. Wiley Online Library.

Lum, G., Solarz, D.E., Farney, L., 2006. False positive cardiac troponin results in patients without acute myocardial infarction. Laboratory Medicine 37(9), 546-550.

Matharu, Z., Bandodkar, A.J., Sumana, G., Solanki, P.R., Ekanayake, E.M., Kaneto, K., Gupta, V., Malhotra, B., 2009. Low density lipoprotein detection based on antibody immobilized self-assembled monolayer: investigations of kinetic and thermodynamic properties. The Journal of Physical Chemistry B 113(43), 14405-14412.

Moon, S., Kim, D.J., Kim, K., Kim, D., Lee, H., Lee, K., Haam, S., 2010. Surface-enhanced plasmon resonance detection of nanoparticle-conjugated DNA hybridization. Applied optics 49(3), 484-491.

Nakaminami, T., Ito, S.-i., Kuwabata, S., Yoneyama, H., 1999. A biomimetic phospholipid/alkanethiolate bilayer immobilizing uricase and an electron mediator on an Au electrode for amperometric determination of uric acid. Analytical Chemistry 71(19), 4278-4283.
Orazem, M.E., Tribollet, B., 2011. Electrochemical impedance spectroscopy. John Wiley & Sons.
Otto, A., 1968. Excitation of nonradiative surface plasma waves in silver by the method of frustrated total reflection. Zeitschrift Fur Physik 216(4), 398-410.

Pandey, C.M., Singh, R., Sumana, G., Pandey, M., Malhotra, B., 2011. Electrochemical genosensor based on modified octadecanethiol self-assembled monolayer for Escherichia coli detection. Sensors and Actuators B: Chemical 151(2), 333-340.

Pandey, C.M., Sumana, G., Sood, K., Malhotra, B., 2010. Electrochemical studies of cystine modified self-assembled monolayer for Escherichia coli detection. Thin Solid Films 519(3), 1178-1183.

Pandey, C.M., Sumana, G., Tiwari, I., 2014a. Copper oxide assisted cysteine hierarchical structures for immunosensor application. Applied Physics Letters 105(10), 103706.

Pandey, C.M., Sumana, G., Tiwari, I., 2014b. Nanostructuring of hierarchical 3D cystine flowers for high-performance electrochemical immunosensor. Biosensors and Bioelectronics 61, 328-335.

Pawula, M., Altintas, Z., Tothill, I.E., 2016. SPR detection of cardiac troponin T for acute myocardial infarction. Talanta 146, 823-830.

Periyakaruppan, A., Gandhiraman, R.P., Meyyappan, M., Koehne, J.E., 2013. Label-free detection of cardiac troponin-I using carbon nanofiber based nanoelectrode arrays. Analytical Chemistry 85(8), 3858-3863.

Pumera, M., 2010. Graphene-based nanomaterials and their electrochemistry. Chemical Society Reviews 39(11), 4146-4157.

Ruan, C., Yang, L., Li, Y., 2002. Immunobiosensor chips for detection of Escherichia c oli O157: H7 using electrochemical impedance spectroscopy. Analytical Chemistry 74(18), 4814-4820.

Sigal, G.B., Bamdad, C., Barberis, A., Strominger, J., Whitesides, G.M., 1996. A self-assembled monolayer for the binding and study of histidine-tagged proteins by surface plasmon resonance. Analytical Chemistry 68(3), 490-497.

Srivastava, S., Ali, M.A., Umrao, S., Parashar, U.K., Srivastava, A., Sumana, G., Malhotra, B., Pandey, S.S., Hayase, S., 2014. Graphene oxide-based biosensor for food toxin detection. Applied biochemistry and biotechnology 174(3), 960-970.

Srivastava, S., Kumar, V., Ali, M.A., Solanki, P.R., Srivastava, A., Sumana, G., Saxena, P.S., Joshi, A.G., Malhotra, B., 2013. Electrophoretically deposited reduced graphene oxide platform for food toxin detection. Nanoscale 5(7), 3043-3051.

Tiwari, I., Singh, M., Pandey, C.M., Sumana, G., 2015. Electrochemical genosensor based on graphene oxide modified iron oxide–chitosan hybrid nanocomposite for pathogen detection. Sensors and Actuators B: Chemical 206, 276-283.

Wang, Z., Zhou, X., Zhang, J., Boey, F., Zhang, H., 2009. Direct electrochemical reduction of single-layer graphene oxide and subsequent functionalization with glucose oxidase. The Journal of Physical Chemistry C 113(32), 14071-14075.

Wei, J., Mu, Y., Song, D., Fang, X., Liu, X., Bu, L., Zhang, H., Zhang, G., Ding, J., Wang, W., 2003. A novel sandwich immunosensing method for measuring cardiac troponin I in sera. Analytical biochemistry 321(2), 209-216.

Zapp, E., da Silva, P.S.r., Westphal, E., Gallardo, H., Spinelli, A., Vieira, I.C., 2014. Troponin T Immunosensor Based on Liquid Crystal and Silsesquioxane-Supported Gold Nanoparticles. Bioconjugate chemistry 25(9), 1638-1643.

Zhang, B., Morales, A.W., Peterson, R., Tang, L., Ye, J.Y., 2014. Label-free detection of cardiac troponin I with a photonic crystal biosensor. Biosensors and Bioelectronics 58, 107-113.

Zhou, M., Zhai, Y., Dong, S., 2009. Electrochemical sensing and biosensing platform based on chemically reduced graphene oxide. Analytical Chemistry 81(14), 5603-5613.